

1 **The first-in-class ERK inhibitor ulixertinib shows promising activity in MAPK-**
2 **driven pediatric low-grade glioma models**

3 Romain Sigaud *, Lisa Rösch *, Charlotte Gatzweiler *, Julia Benzel *, Laura von
4 Soosten *, Heike Peterziel, Florian Selt, Sara Najafi, Simay Ayhan, Xenia F. Gerloff,
5 Nina Hofmann, Isabel Büdenbender, Lukas Schmitt, Kathrin I. Foerster, Jürgen
6 Burhenne, Walter E. Haefeli, Andrey Korshunov, Felix Sahm, Cornelis M. van
7 Tilburg, David T.W. Jones, Stefan M. Pfister, Deborah Knoerzer, Brent L. Kreider,
8 Max Sauter *, Kristian W. Pajtler *, Marc Zuckermann *, Ina Oehme *, Olaf Witt *, Till
9 Milde *

10 Hopp Children's Cancer Center Heidelberg (KiTZ), Heidelberg, Germany (R.S., L.R.,
11 C.G., J.B., L.vS., H.P., F.S., S.N., S.A., X.F.G., N.H., I.B., L.S., C.M.vT., D.T.W.J.,
12 S.M.P., K.W.P., M.Z., I.O., O.W., T.M.); Clinical Cooperation Unit Pediatric
13 Oncology, German Cancer Research Center (DKFZ) and German Consortium for
14 Translational Cancer Research (DKTK), Heidelberg, Germany (R.S., L.R., C.G., H.P.,
15 F.S., S.N., S.A., X.F.G., I.B., C.M.vT., I.O., O.W., T.M.); Faculty of Biosciences,
16 Heidelberg University, Heidelberg, Germany (L.R., J.B., L.vS., S.A.); Faculty of
17 Medicine, Heidelberg University, Heidelberg, Germany (C.G.); Division of Pediatric
18 Neurooncology, German Cancer Consortium (DKTK), German Cancer Research
19 Center (DKFZ), Heidelberg, Germany (J.B., S.M.P., K.W.P.); Preclinical Modeling
20 Group, German Cancer Research Center (DKFZ), Heidelberg, Germany (L.vS., N.H.,
21 M.Z.); Division of Pediatric Glioma Research, German Cancer Research Center
22 (DKFZ), Heidelberg, Germany (L.vS., D.T.W.J.); KiTZ Clinical Trial Unit, Department
23 of Pediatric Oncology, Hematology, Immunology and Pulmonology, Heidelberg
24 University Hospital, Heidelberg, Germany (F.S., S.N., S.A., X.F.G., C.M.vT., S.M.P.,
25 K.W.P., O.W., T.M.); Pediatric Soft Tissue Sarcoma Research Group, German
26 Cancer Research Center (DKFZ), Heidelberg, Germany (L.S.); Department of Clinical
27 Pharmacology and Pharmacoepidemiology, Heidelberg University Hospital,
28 Heidelberg, Germany (K.I.F., J.B., W.E.H., M.S.); Department of Neuropathology,
29 Heidelberg University Hospital, Heidelberg, Germany (A.K.; F.S.); Clinical
30 Cooperation Unit Neuropathology, German Consortium for Translational Cancer
31 Research (DKTK), German Cancer Research Center (DKFZ), Heidelberg, Germany
32 (A.K., F.S.); BioMed Valley Discoveries Inc., Kansas City, Missouri (D.K., B.K.).

33

34 *shared first or last authors

35

36

SUPPLEMENTARY MATERIALS

37

38 **Supplementary Methods**

39 **Cell culture**

40 Cell lines were authenticated using Multiplex Cell Authentication,¹ and purity was
41 validated using the Multiplex cell Contamination Test,² both performed by
42 Multiplexion (Heidelberg, Germany).

43 **Drug treatments *in vitro***

44 All three cell lines were seeded at the same time (for seeding densities, see
45 Supplementary Table S1), left for five days to allow the repression of the SV40 Large
46 T antigen in the DKFZ-BT66_OFF cells, and subsequently treated with the indicated
47 drugs (see Supplementary Table S8) using a D300e Digital Dispenser (Tecan Life
48 Sciences). 1/2 Log distribution was used to cover a range of concentrations from
49 10 μ M to 1 nM. Each condition was done in technical duplicates for three
50 independent biological replicates. Raw values were normalized to their corresponding
51 death control (250 nM STS for metabolic activity; 10 μ M trametinib for MAPK reporter
52 assay) and healthy control (DMSO), and used to calculate IC₅₀. Normalized data was
53 plotted onto a 4-parameter dose response model

54 **High content microscopy (HCM)**

55 For BT40 the nuclear stain Hoechst33342 was used to define whole nuclei and
56 fragmented nuclei as readouts of total cell number and dead cells respectively.
57 TMRE stains active mitochondria and was thus used to define viable cells, while the
58 staining of active caspases with CellEvent Caspase3/7 detected apoptotic cells.
59 For DKFZ-BT66 the total cell number was determined equivalently to BT40. DRAQ7
60 is a nuclear stain, which cannot pass the cell membrane of living cells. Thus, dead
61 cells with damaged membranes were determined as the ratio of DRAQ7 positive cells

62 to Hoechst3342 positive cells. Finally, cell size was determined as area of the live-
63 cell stain calceinAM and expressed as change from DMSO.

64 All readouts were normalized to healthy control (DMSO) and death control (1000 nM
65 staurosporine).

66 For Cell Prolifer pipelines details, see Supplementary Table S9.

67 **Synergy analysis**

68 For a given readout, when the dimensional change upon single treatment was
69 concordant with an inhibitory effect for both combined drugs, synergy was calculated
70 with the Loewe model. When the dimensional change upon single treatment was
71 opposite to an inhibitory effect for one of the combined drugs, and if drug
72 independence could be assumed, synergy was calculated with the Bliss
73 independence model. When the dimensional change upon single treatment was
74 absent for one of the combined drugs, synergy was calculated with the highest single
75 agent (HSA) model. When the dimensional change upon single treatment was
76 opposite to an inhibitory effect for both combined drugs, synergy calculation was not
77 applied. See Supplementary Figure S21 for details on what synergy model was used
78 in which readout/cell line.

79 ***In vitro* on-target activity validation**

80 Samples were washed twice with ice-cold PBS. For Western blot, cell were lysed in a
81 lysis buffer containing 62.5 mM Tris/HCl (Carl Roth, cat. no. 9090.2) pH 6.8, 2% SDS
82 (Carl Roth, cat. no. 2326.1), 10% glycerol (Sigma-Aldrich, cat. no. 33226), 1 mM dTT
83 (AppliChem, cat. no. A1101), phosphatase inhibitor (PhosphoSTOP, Merck, cat. no.
84 4906837001), protease inhibitor (cOmplete™ Protease Inhibitor Cocktail, Merck, cat.
85 no. 11697498001). For reverse-phase protein array, cell were lysed in a lysis buffer

86 containing 45% 2xSDS, 45%T-PER (Thermo Scientific, cat. no. 78510), 10% TCEP
87 (Thermo Scientific, cat. no. 77720)). For immunoprecipitation, cells were lysed in a
88 lysis buffer containing 300 mM Tris/HCl (Carl Roth, cat. no. 9090.2), 120 mM NaCl
89 (ThermoFisher Scientific, BP358-1), 10% glycerol (Sigma-Aldrich, cat. no. 33226),
90 2 mM EDTA (GERBU Biotechnik GmbH, 1034), 2 mM KCl (Carl Roth, 6781.1),
91 1% Triton X-100 (AppliChem, A4975.0500), protease inhibitor (cOmplete™ Protease
92 Inhibitor Cocktail, Merck, cat. no. 11697498001). Antibodies were crosslinked to
93 Dynabeads™ using freshly dissolved 20 mM dimethyl-pimelimidate (DMP) in 0.2 M
94 triethanolamine buffer.

95 **Zebrafish embryo toxicity assay, xenotransplantation, and treatment**

96 *Zebrafish toxicity assay*

97 Zebrafish embryos were treated 48 hours post fertilization (hpf) in 48-well plates (cat.
98 no. 351178, Corning) containing E3 buffer supplemented with 0.2nM 1-phenyl-2-
99 thiourea (PTU buffer) and increasing concentrations as indicated. As determined by
100 us and others^{29,36,37}, effective concentrations usually are up to 10-to 20-fold higher in
101 the zebrafish embryo xenograft model than in cell culture studies. Thus, drugs in
102 concentrations 10 times higher than the corresponding *in vitro* metabolic IC₅₀ rounded
103 to the closest power of ten were applied to the embryo-containing buffer solution
104 (e.g.: IC₅₀ Ulixertinib = 62nM; closest power of 10 = 100nM; 10-fold = 1 μM). During
105 treatment (48 hpf - 120 hpf) the embryos were kept at 34°C. Imaging was performed
106 at 72 hpf and 120 hpf using a stereo microscope (Leica). Zebrafish embryos were
107 assessed for signs of toxicity (morphological changes, death, reaction to outside
108 stimuli). A maximum tolerated dose (MTD) was determined as the highest tested
109 concentration without manifestations of toxicity.

111 *Zebrafish embryos xenografts imaging*

112 After transplantation, zebrafish embryos were distributed in 48-well plates containing
113 1-phenyl-2-thiourea (PTU) buffer and kept at 34 °C. 24 h post injection (hpi), embryos
114 were treated for 48h with drugs diluted in PTU buffer, as indicated. Imaging was done
115 at 24 hpi and 72 hpi. Zebrafish embryos were anesthetized with tricaine (MS-222,
116 Ethyl 3-aminobenzoate methanesulfonate, 0.02% (w/v), Sigma-Aldrich) and either
117 transferred (one embryo/well) to Hashimoto 96-well zebrafish imaging plates
118 (Funakoshi Co., Ltd., Tokyo, Japan) for imaging with the ImageXpress Micro
119 Confocal High Content Microscope (Molecular Devices) at a temperature of 32-
120 34 °C, or put into chambered coverslips (ibidi, Martinsried, Germany) for imaging with
121 the Zeiss LSM 710 confocal microscope (Zeiss, Oberkochen, Germany) equipped
122 with the 10×/0.3 EC Plan-Neofluar and 20×/0.8 Plan-Apochromat objectives, Argon
123 514 nm laser line for Dil, standard PMT for fluorescence detection and T-PMT for
124 transmitted light controlled by ZEN software (Zeiss). A Cy3-channel was used for the
125 detection of RFP.

126

127 *Zebrafish embryos treatment*

128 Treatment response of tumor growth was captured by tumor volume change from
129 baseline (day one to day three post-implantation). To determine tumor progression,
130 we used an in-house macro for FIJI software, as described previously.³ Best
131 response was evaluated according to Response Evaluation Criteria in Solid Tumors
132 (RECIST) 1.1 adopted for zebrafish tumors:³ progressive disease (PD), at least a
133 20% increase in tumor volume; partial response (PR), at least a 30% decrease in
134 tumor volume. A PD/PR ratio was used to assess treatment's efficacy.

135 **BT40 xenograft mouse model, treatment, and imaging**

136 Drugs and solvents were used as indicated in Supplementary Table S10.

137 **Pharmacokinetic study**

138 After three weeks, mice were randomly split into two cohorts based on weight and
139 ranked luciferase signal. The time window was covered by seven groups (four dosed
140 mice per group) with four blood collection time points per group, due to blood volume
141 restrictions for sampling within 24 h. Full blood samples were transferred into EDTA
142 tubes (cat. no. 77003, KABE) and centrifuged at 3,000x g for 10 min to generate
143 plasma samples, which were stored at -80 °C until analysis. For brain tissue
144 determinations, tissue samples were harvested as indicated, and stored at -80 °C
145 until analysis. Brain tissue samples were homogenized using a Bead Ruptor 4
146 homogenizer (Omni International Inc) in acetonitrile (ACN)/water (1/19, v/v) + 0.5%
147 triton X and 0.1% formic acid (FA) (100 mg brain tissue/mL) in 2.0 mL tubes
148 containing ~25 glass beads (0.75-1 mm; cat. no. A554.1, Carl Roth GmbH) for 2 ×
149 1 min.

150 **Ulixertinib and navitoclax bioanalysis**

151 *UPLC-MS/MS quantification assay*

152 Microdialysate, plasma, and brain tissue concentrations were measured using a
153 validated ultra-performance liquid chromatography – tandem mass spectrometry
154 (UPLC-MS/MS) quantification assay following the pertinent guidelines of the US FDA
155 and EMA.^{4,5} Each of four performed validation runs included blank and internal
156 standard controls, seven calibration samples (two-fold), and four quality control
157 concentrations (six-fold). The assays fully complied with the applicable
158 recommendations of the US FDA and EMA on bioanalytical method validation.

159 *Ulixertinib quantification*

160 Optimized MS/MS parameters for the detection of ulixertinib can be found in
161 Supplementary Table S11. The calibrated range for ulixertinib quantification was 1 –
162 1,000 ng/mL (corresponding to 10 – 10,000 ng/g for brain tissue), which was
163 additionally extended to 0.1 – 100 µg/mL, all showing linear regression coefficients >
164 0.99. Overall accuracies (inter- and intraday) were 87.0 to 109.3% with
165 corresponding precision < 6.7%. A Xevo-TQ-S tandem mass spectrometer (Waters,
166 Milford, MA, USA) coupled to an I-class UPLC (Waters) and equipped with heated
167 electrospray ionization source was used for quantification with selected reaction
168 monitoring using collision-induced dissociation with argon in the positive ion mode.
169 Chromatographic separation was performed on a BEH C18 column (50 × 2.1 mm;
170 1.7 µm; Waters) with a gradient from 5 to 95% acetonitrile (ACN) + 0.1% FA in 1.5
171 min (corresponding decrease of aqueous eluent: 19/1 H₂O/ACN + 0.1% FA) at a flow
172 rate of 0.5 mL/min. Microsamples (25 µL) were spiked with internal standard
173 (Ulixertinib-D6) and 200 µL of borate buffer (pH 9). Ulixertinib was extracted with 1
174 mL of tert-butyl methyl ether. After evaporation of 200 µL of the ether phase, extracts
175 were dissolved in 400 µL ACN/H₂O (1/3) + 0.1% formic acid and 5 µL were injected
176 for analysis.

177 Navitoclax quantification

178 Optimized MS/MS parameters for the detection of navitoclax can be found in
179 Supplementary Table S12. The calibrated range was 0.05 – 50 ng/mL
180 (corresponding to 0.5 – 500 ng/g for tumor tissue), all showing linear regression
181 coefficients > 0.99. Overall accuracies (inter- and intraday) were 94.7 to 110.8% with
182 corresponding precision < 9.8 %. A Xevo-TQ-XS tandem mass spectrometer
183 (Waters, Milford, MA, USA) coupled to an Acquity classic UPLC (Waters) and
184 equipped with heated electrospray ionization source was used for quantification with

185 selected reaction monitoring using collision-induced dissociation with argon in the
186 positive ion mode. Chromatographic separation was performed on a BEH C18
187 Peptide column 300 Å (50 × 2.1 mm; 1.7 µm; Waters) with a gradient from 20 to 95%
188 ACN + 0.1% FA in 1.9 min (corresponding decrease of aqueous eluent: 19/1
189 H₂O/ACN + 0.1% FA) at a flow rate of 0.5 mL/min. Samples (100 µL) were spiked
190 with internal standard (venetoclax) and extracted by protein precipitation using 300
191 µL of ACN. After partial evaporation of the separated supernatant and addition of 50
192 µL of H₂O + 0.1% formic acid, 20 µL were injected for UPLC-MS/MS analysis.

193

194 *Sample preparation for ulixertinib on-target analysis in vivo (DUSP6 Western blot)*

195 Tissue samples were weighed, resuspended in 1:10 w/v lysis buffer (49% SDS
196 buffer, 50% T-PER buffer, 10mM DTT, phosphatase inhibitor (PhosphoSTOP, Merck,
197 cat. no. 4906837001), protease inhibitor (cOmplete™ Protease Inhibitor Cocktail,
198 Merck, cat. no. 11697498001)) and disrupted using a benchtop tissue homogenizer.
199 The resulting lysates were centrifuged at 10,000 × g for 5 minutes and the
200 supernatant was collected. The protein concentration of each lysate was determined
201 using the Pierce™ BCA Protein Assay kit (ThermoFisher Scientific, cat. no. 23227)
202 for subsequent Western blot analysis.

203 ***In vivo preclinical study***

204 After two weeks of tumor development, animals were distributed into six treatment
205 groups (n=8 per group) based on their ranked luciferase signal according to the
206 following pattern: “ABCDEFEDCBAA...”. Ulixertinib (75 mg/kg) and the vehicle were
207 administered via oral gavage every 12 h. Navitoclax (100 mg/kg) was administered
208 via oral gavage every 24 h. Vinblastine (0.5 mg/kg) was injected intraperitoneally

209 every 72 h. During the treatment period, animals were weighed every second day
210 and tumor development was monitored twice per week by bioluminescence imaging.

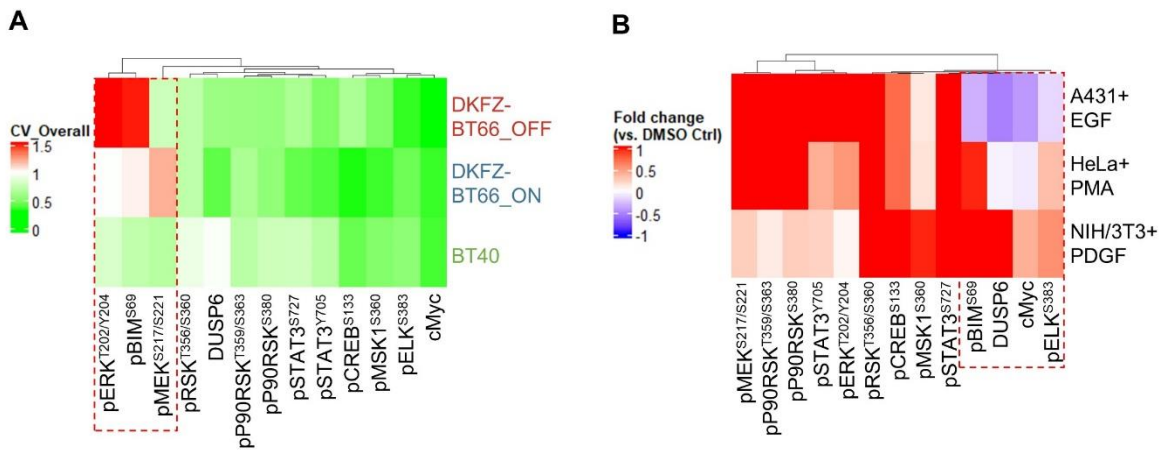
211 **Statistical analysis and graphical representations**

212 IC50 calculation was performed using GraphPad Prism 5 software (Version 5.01,
213 GraphPad Software Inc., San Diego, USA). RStudio (R Version 1.4.1103) was used
214 for calculation of ANOVA followed by Tukey's honest significant test. Synergy scores
215 were computed using the online platform SynergyFinderPlus
216 (<https://synergyfinder.org/>)³² (matrix design), and the R package drugCombo 1.1.1
217 (ray design). Consensus rankings were generated with the R package challengeR³⁷
218 using average ranks. Quantification of Western blot bands was conducted using
219 ImageJ (version 1.53e, Wayne Rasband and co., NIH). Calibration curves for the
220 ulixertinib bioanalysis were determined with 1/x² weighted linear regression using
221 peak area ratios of the analyte to IS, using the software TargetLynx (V4.2, Waters,
222 Milford, USA). Plasma pharmacokinetics were determined with the software Kinetica
223 (v 5.0, Thermo Fisher Scientific, Philadelphia, USA). Bioluminescence measurements
224 were analyzed with the LivingImage software (v4.5.2, Caliper Life Sciences,
225 Massachusetts, USA). Survival curves were generated in R using the survminer
226 package. Significance between survival curves were calculated using the log-rank
227 test in GraphPad Prism 8 software (Version 8.0.2.263, GraphPad Software Inc., San
228 Diego, USA).

229

230 **Supplementary Figures**

Supplementary Fig. S1



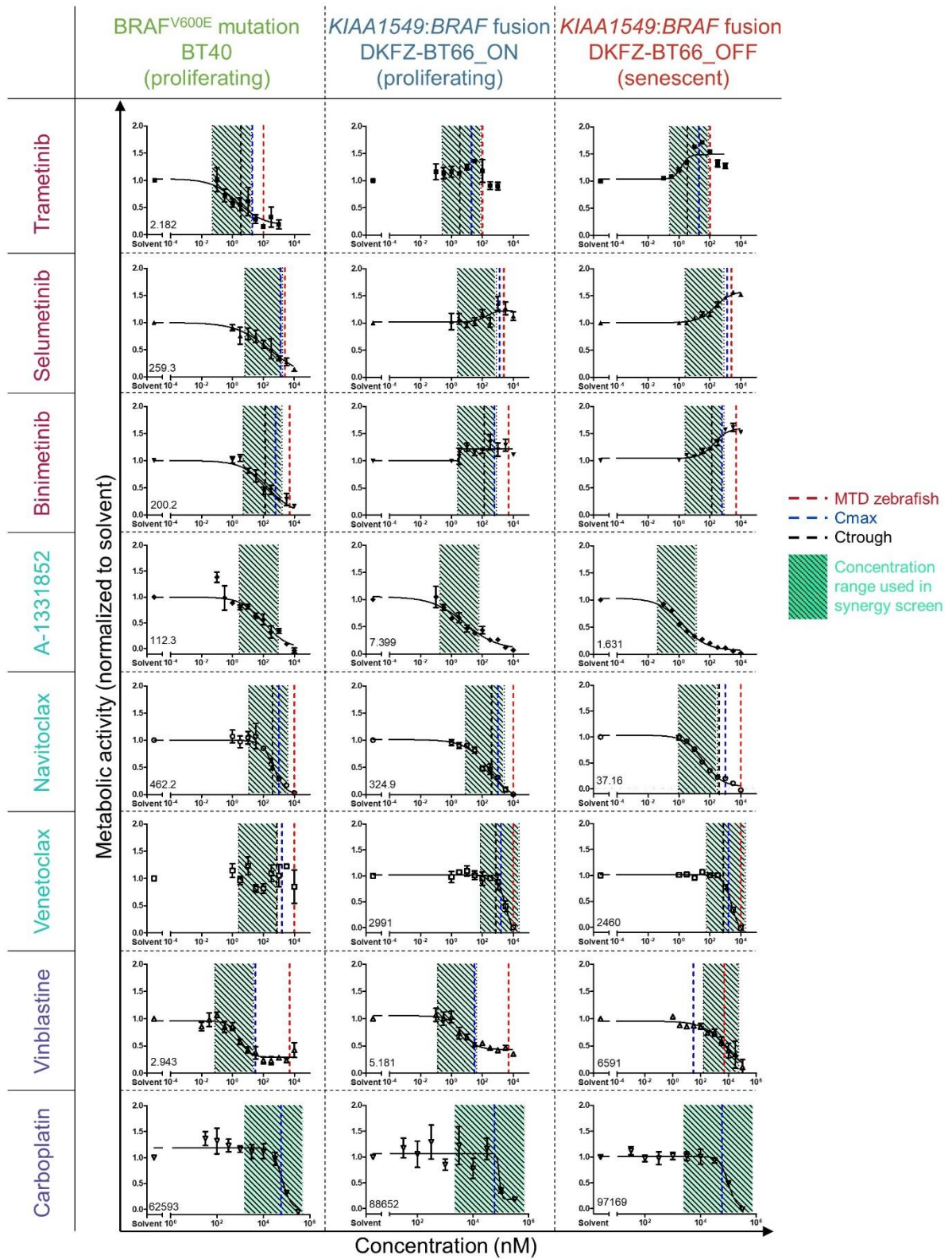
231

232 **Supplementary Fig. S1: Reverse-phase protein array (RPPA) quality**
233 **control**

234 A, Heatmap depicting the coefficient of variation (CV) obtained in the reverse-phase
235 protein array (RPPA) data across biological replicates. Green indicates low variance
236 (CV < 1), red indicates high variance (CV > 1). Red dotted square indicates markers
237 that didn't pass the threshold and were excluded. B, Heatmap depicting
238 phosphoprotein fold change in the indicated control cell lines upon treatment with a
239 MAPK stimulator relative to solvent control. Red indicates an increased fold change,
240 while blue indicates a decreased fold change. Red dotted rectangle indicates
241 markers that showed discrepancy and were excluded. Depicted are data from three
242 biological replicates.

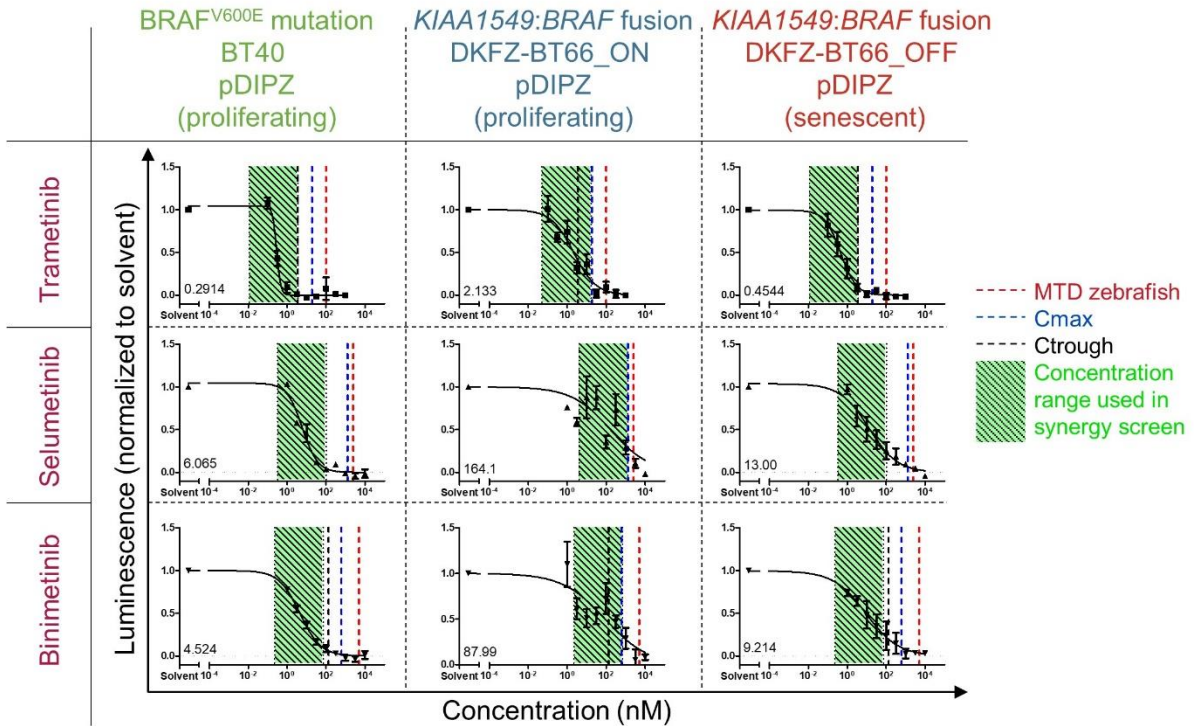
Supplementary Fig. S2

A- Metabolic activity



Supplementary Fig. S2

B- MAPK reporter assay

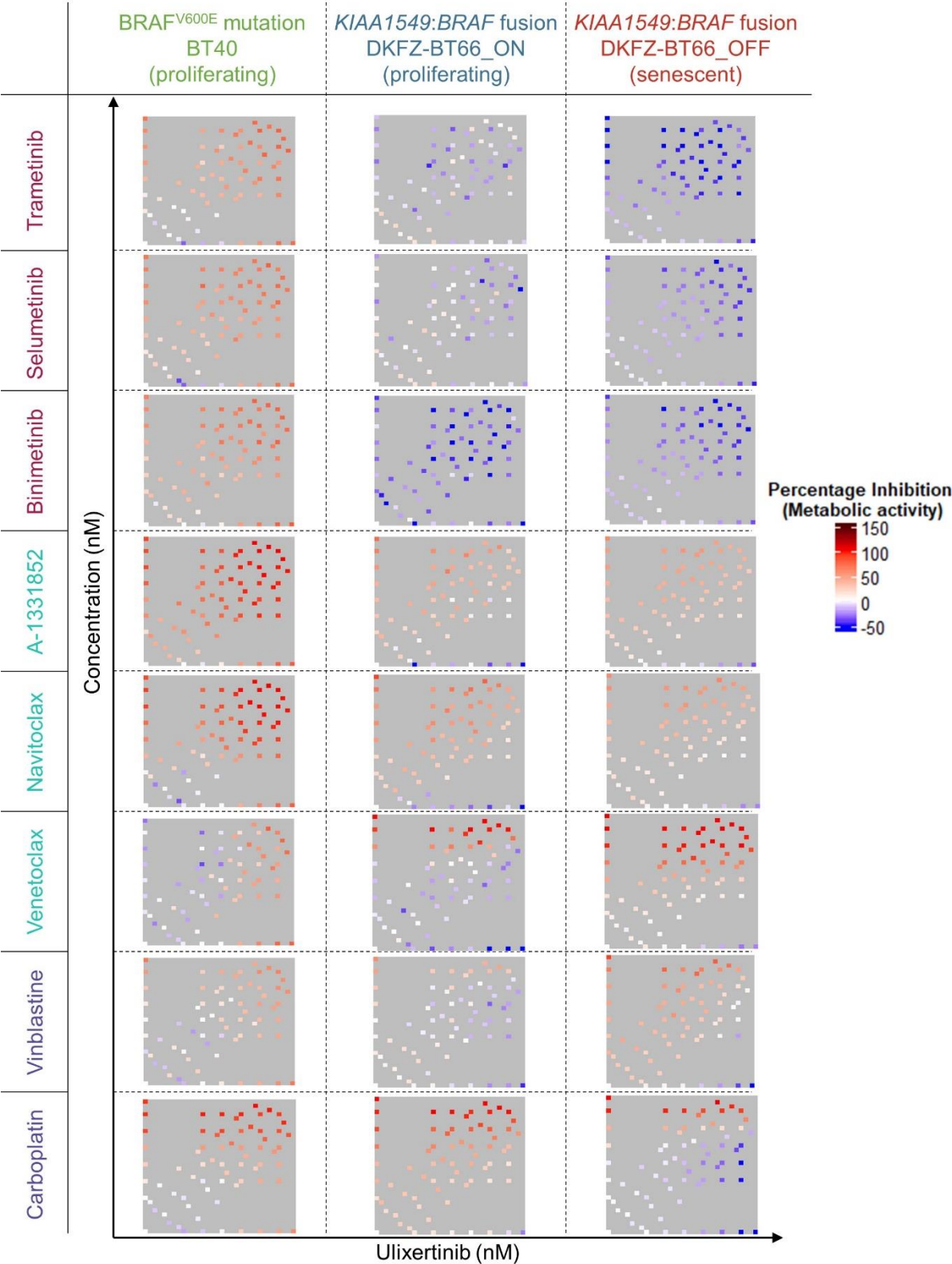


244

245 **Supplementary Fig. S2: IC₅₀ of ulixertinib's combination partners**

246 A, Metabolic activity IC₅₀ (CellTiter-Glo®) measured in BT40, DKFZ-BT66_ON, and
 247 DKFZ-BT66_OFF cells. B, MAPK reporter IC₅₀ measured in BT40, DKFZ-BT66_ON,
 248 and DKFZ-BT66_OFF cells. Each dot represents the mean of three independent
 249 biological replicates. Error bars depict the standard deviation. Published
 250 pharmacokinetic data (C_{max} and C_{trough}, when available), zebrafish embryo
 251 maximum tolerated dose (MTD), and concentrations used in the synergy analysis are
 252 depicted.

Supplementary Fig. S3

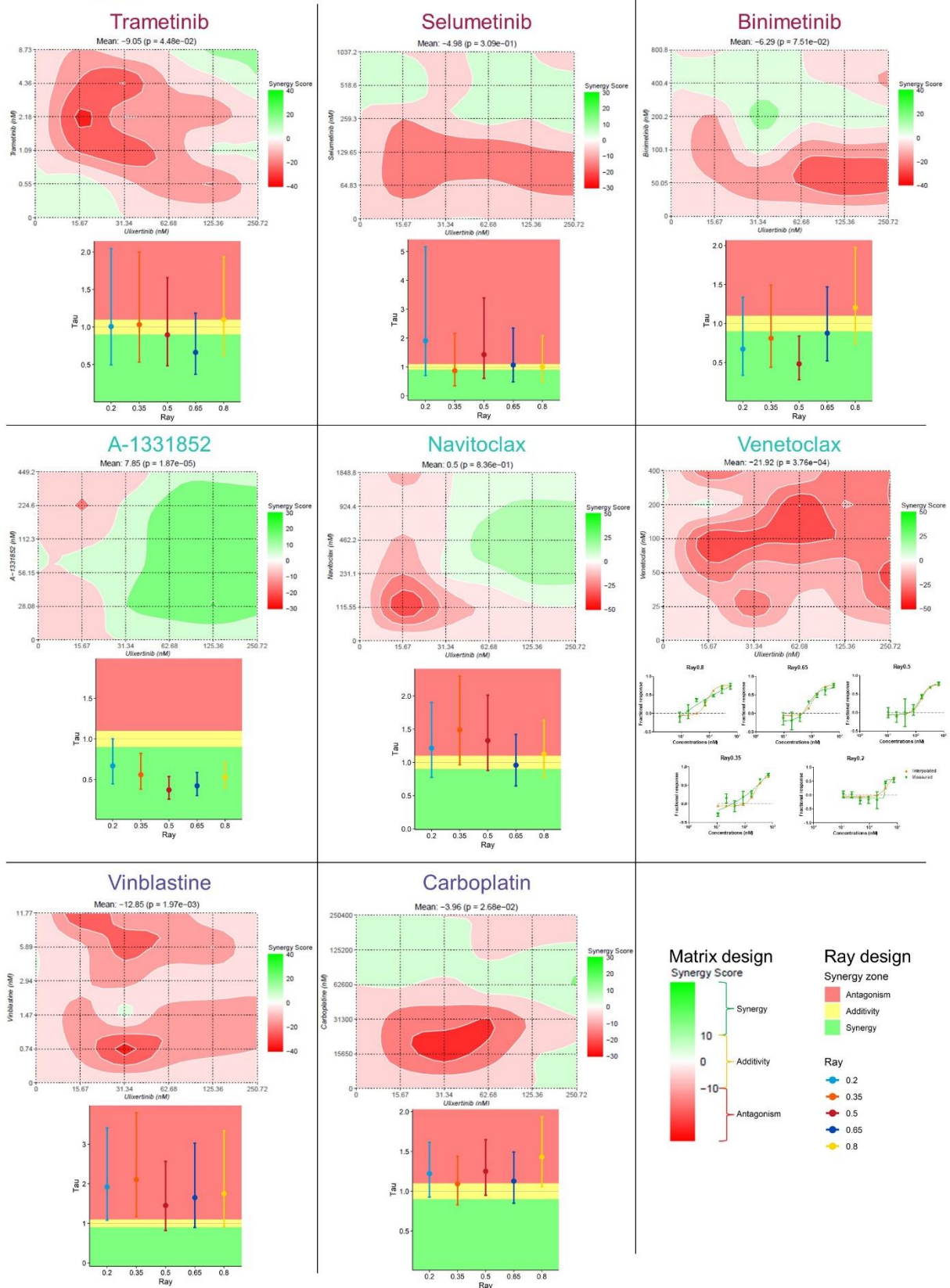


254 **Supplementary Fig. S3: Heatmap of metabolic activity inhibition in the *in***
255 ***vitro* synergy screen**

256 Heatmap depicting the percentage of inhibition of metabolic activity relative to DMSO
257 control in BT40, DKFZ-BT66_ON, and DKFZ-BT66_OFF cells upon combinational
258 treatment of ulixertinib with each combination partner. In the matrix design, each drug
259 was combined using two-fold increment concentration ranges, centered on the
260 corresponding drug's IC₅₀. In the ray design, concentrations were calculated based
261 on each drug's IC₅₀, as described previously (31). Increased inhibition is depicted
262 with red colors, while increased metabolic activity is depicted with blue colors.
263 Depicted are data from three biological replicates.

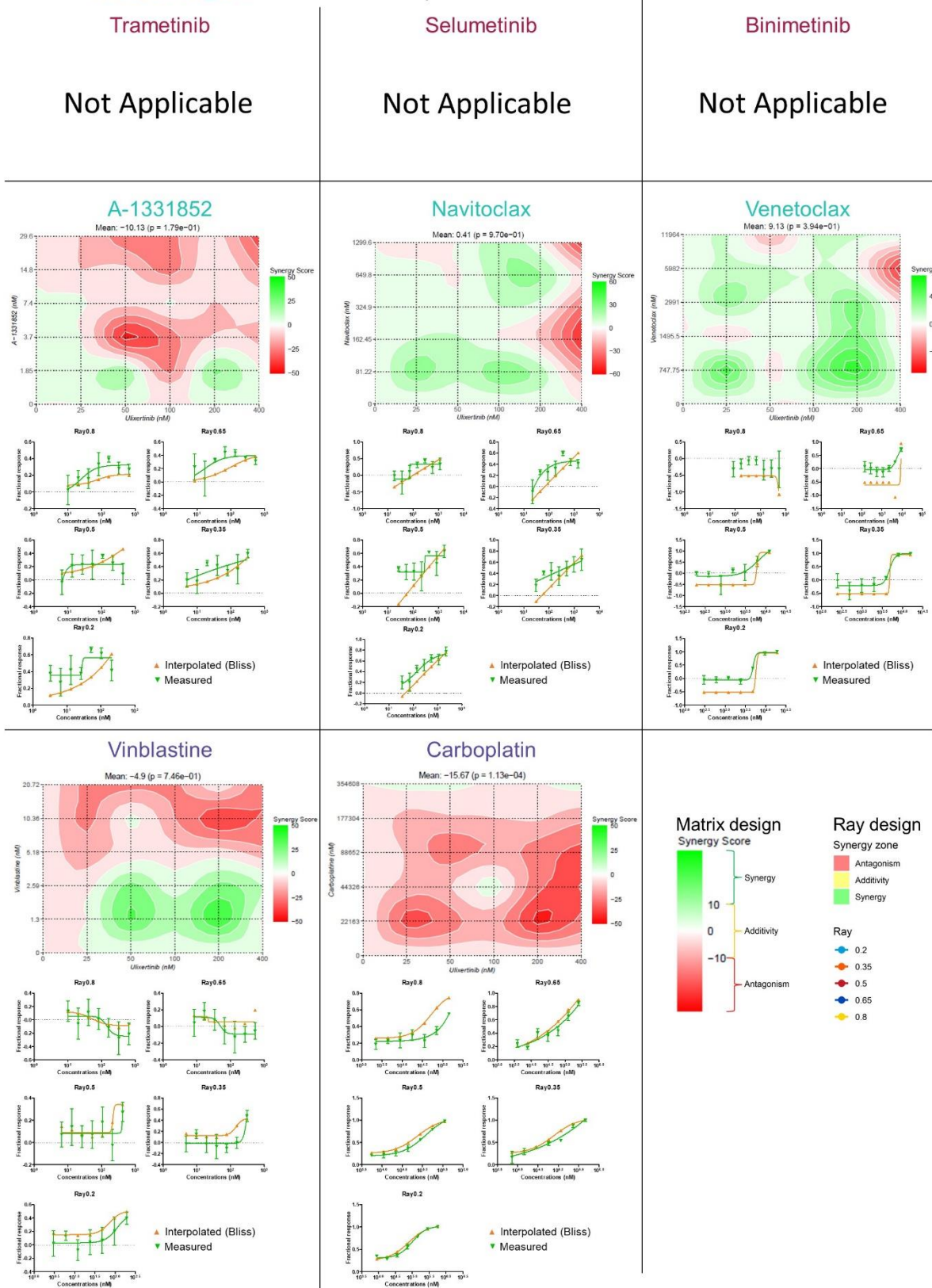
Supplementary Fig. S4

A - BT40 – Metabolic activity



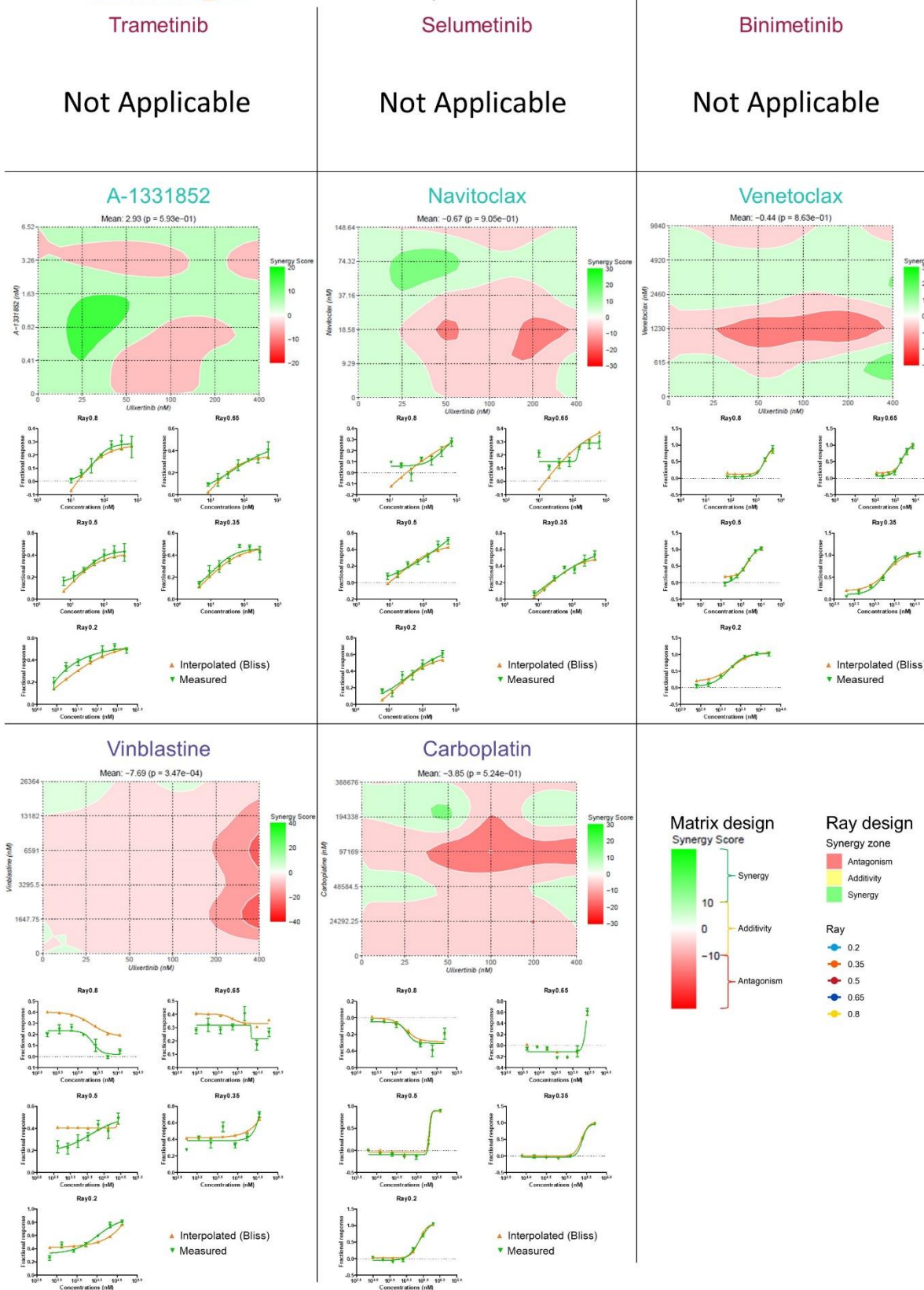
Supplementary Fig. S4

B - DKFZ-BT66_ON – Metabolic activity



Supplementary Fig. S4

C - DKFZ-BT66_OFF – Metabolic activity

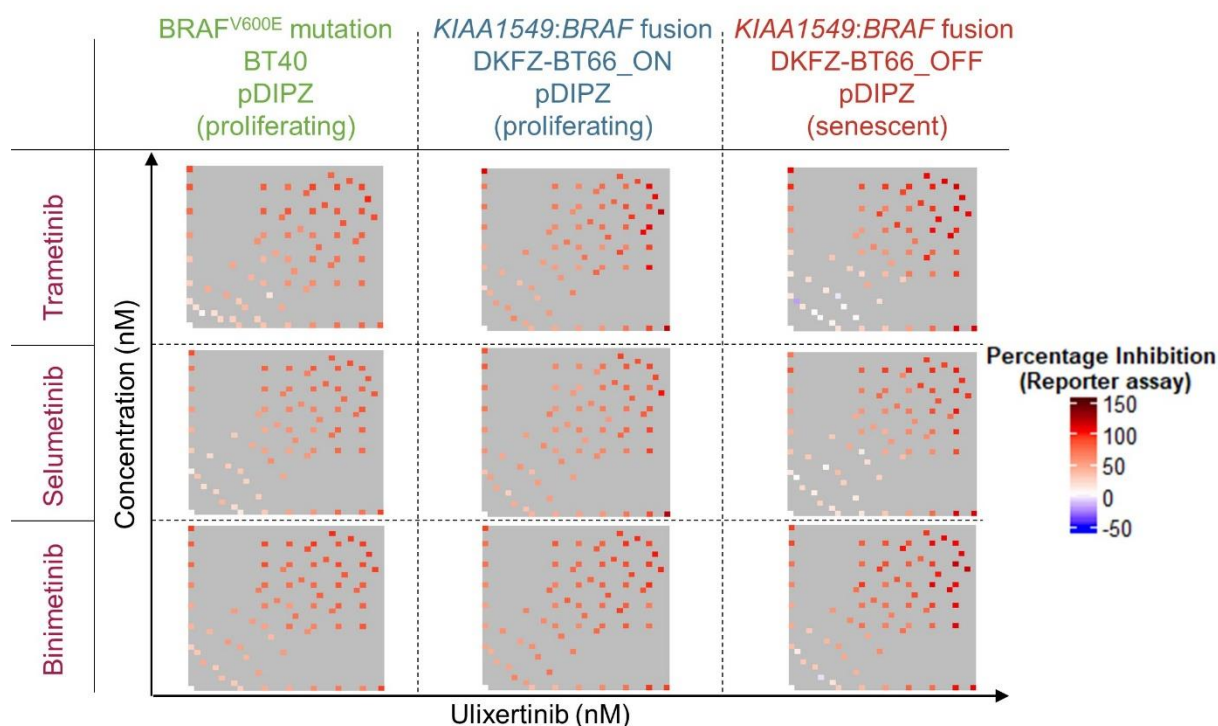


267 **Supplementary Fig. S4: Synergy results for the matrix and ray designs**
268 **using metabolic activity**

269 Synergy maps depicting synergy score across all concentrations tested in the matrix
270 design. Scores above 10 indicate synergy, while scores below -10 indicate
271 antagonism. Dot plots (only where the Loewe model was applied) depict ray synergy
272 scores and bars represent the 95% CI. Scores below 0.9 indicate synergy, scores
273 above 1.1 indicate buffering antagonism, scores above 2 indicate antagonism.
274 Response-curves (only where Bliss independence was applied) depict the expected
275 effect based on the Bliss independence formula (orange curve) and actual measures
276 (green curve). The excess over Bliss score is depicted. Scores above 0 indicate
277 synergy, scores below 0 indicate antagonism. A, Synergy data obtained with
278 metabolic activity in BT40 cells. B, Synergy data obtained in DKFZ-BT66_ON cells.
279 C, Synergy data obtained in DKFZ-BT66_OFF cells. Depicted are data from three
280 biological replicates.

281

Supplementary Fig. S5

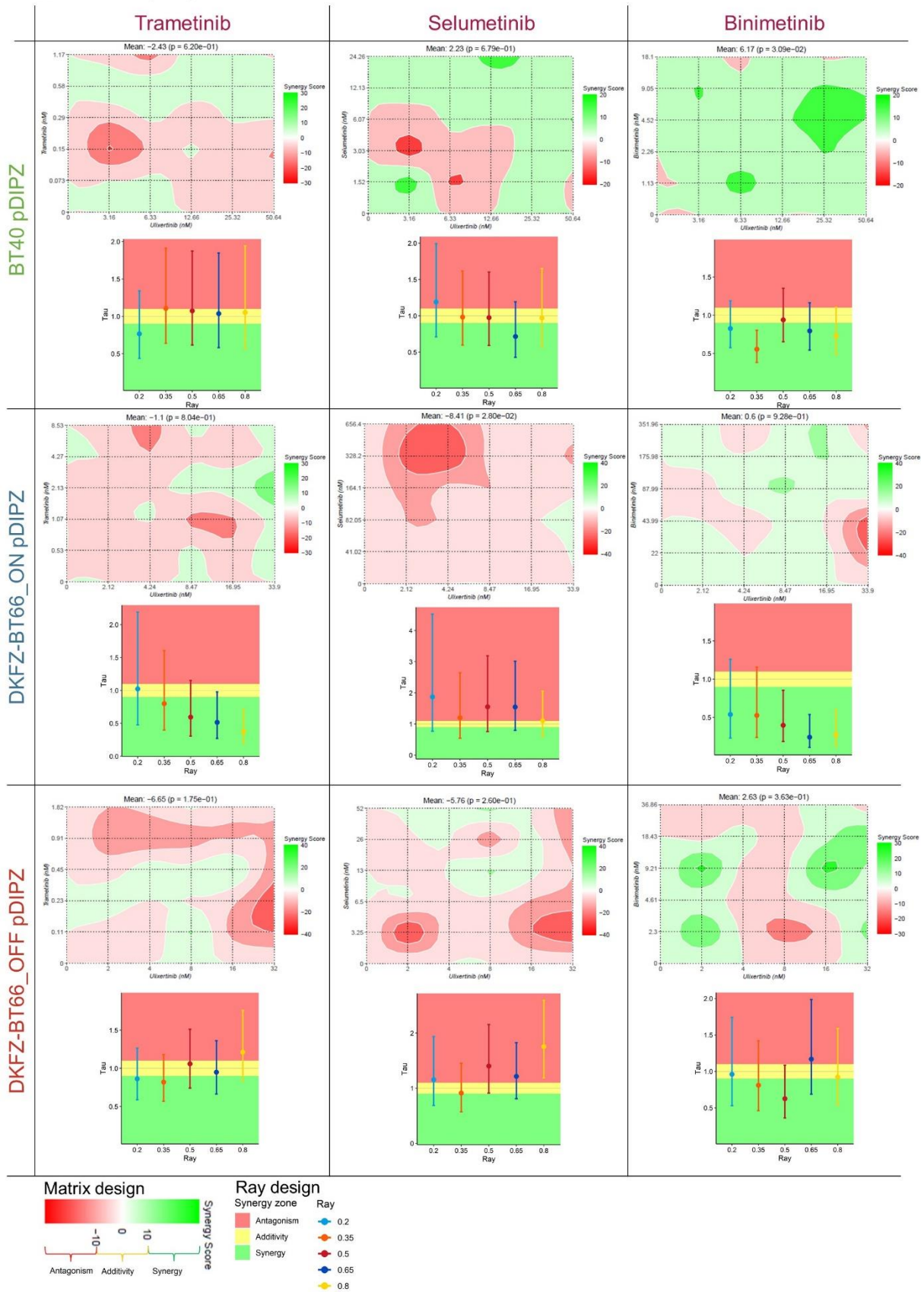


282

283 **Supplementary Fig. S5: Heatmap of MAPK activity (reporter) inhibition in**
 284 **the *in vitro* synergy screen**

285 Heatmap depicting the percentage of inhibition of MAPK pathway activity (assessed
 286 by MAPK reporter assay) relative to DMSO control in BT40, DKFZ-BT66_ON, and
 287 DKFZ-BT66_OFF cells upon combinational treatment with ulixertinib and each
 288 combination partner. In the matrix design, each drug was combined using two-fold
 289 increment concentration ranges, centered on the corresponding drug's IC₅₀. In the
 290 ray design, concentrations were calculated based on each drug's IC₅₀, as described
 291 previously (31). Increased inhibition is depicted with red colors, while increased
 292 metabolic activity is depicted with blue colors. Depicted are data from three biological
 293 replicates.

Supplementary Fig. S6

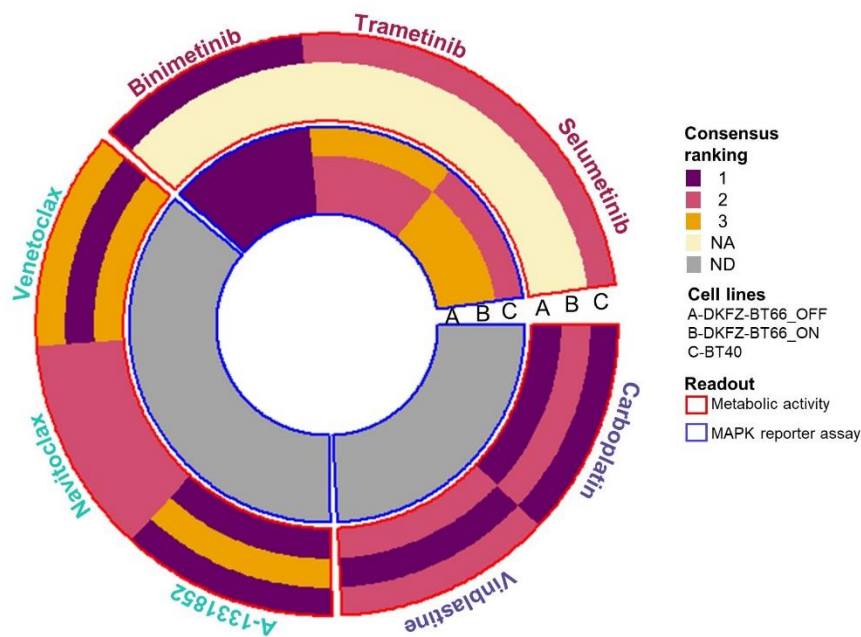


295 **Supplementary Fig. S6: Synergy results for the matrix and ray designs**
296 **using the MAPK reporter assay**

297 Synergy maps depicting synergy scores across all concentrations tested in the matrix
298 design. Scores above 10 indicate synergy, while scores below -10 indicate
299 antagonism. Dot plots depict ray synergy scores and bars represent the 95% CI.
300 Scores below 0.9 indicate synergy, scores above 1.1 indicate buffering antagonism,
301 scores above 2 indicate antagonism. Depicted are data from three biological
302 replicates.

303

Supplementary Fig. S7



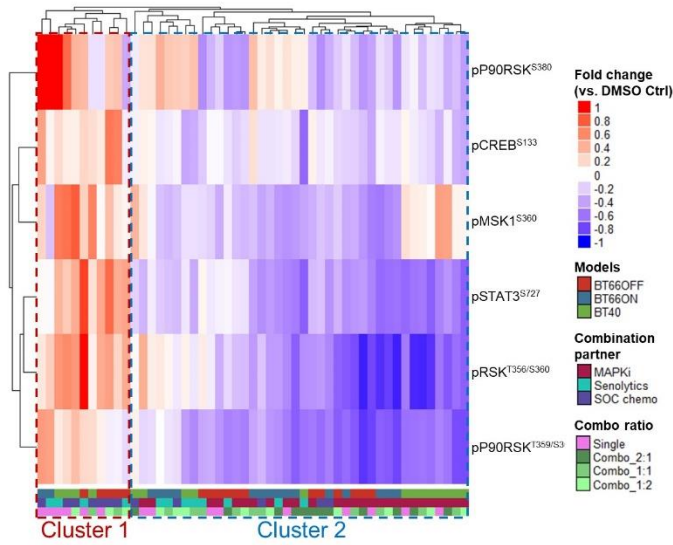
304

305 **Supplementary Fig. S7: Consensus ranking of combination partners in**
 306 **the *in vitro* screen (metabolic activity and MAPK reporter assay)**

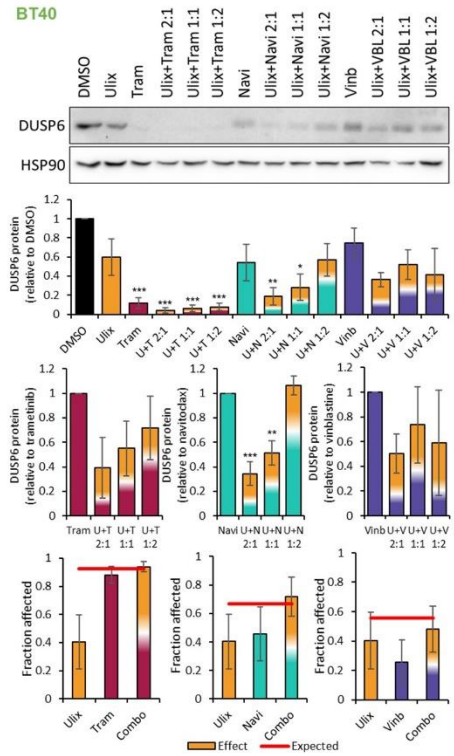
307 Circular heatmap summarizing the individual drug's performance per drug class,
 308 following consensus ranking across synergy metrics. The ranking was calculated for
 309 the DKFZ-BT66_OFF, DKFZ-BT66_ON, and BT40 (designated by A, B, and C
 310 respectively), and for each readout (outermost red rings = metabolic activity;
 311 innermost blue rings = MAPK reporter assay). NA, not applicable due to readout
 312 inconsistency. ND, not determined.

Supplementary Fig. S8

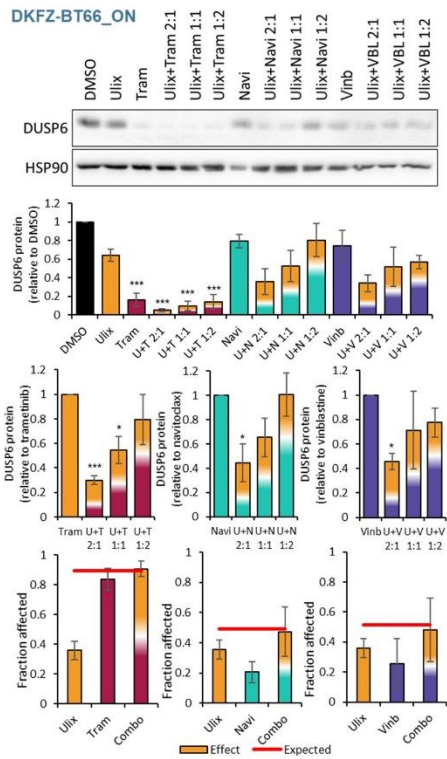
A



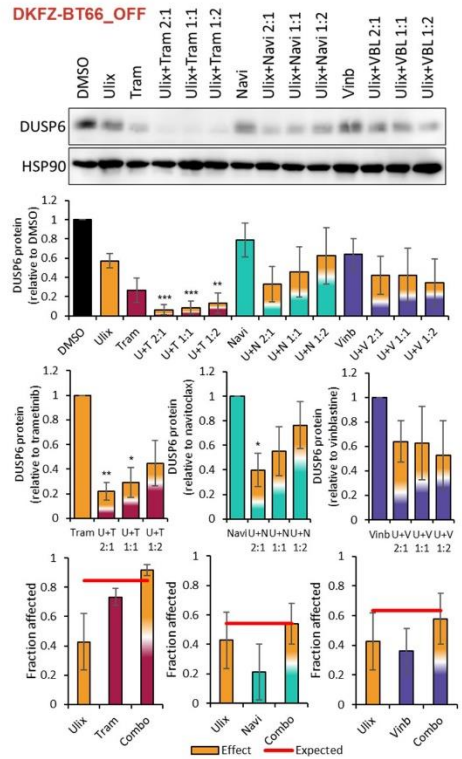
B



C



D

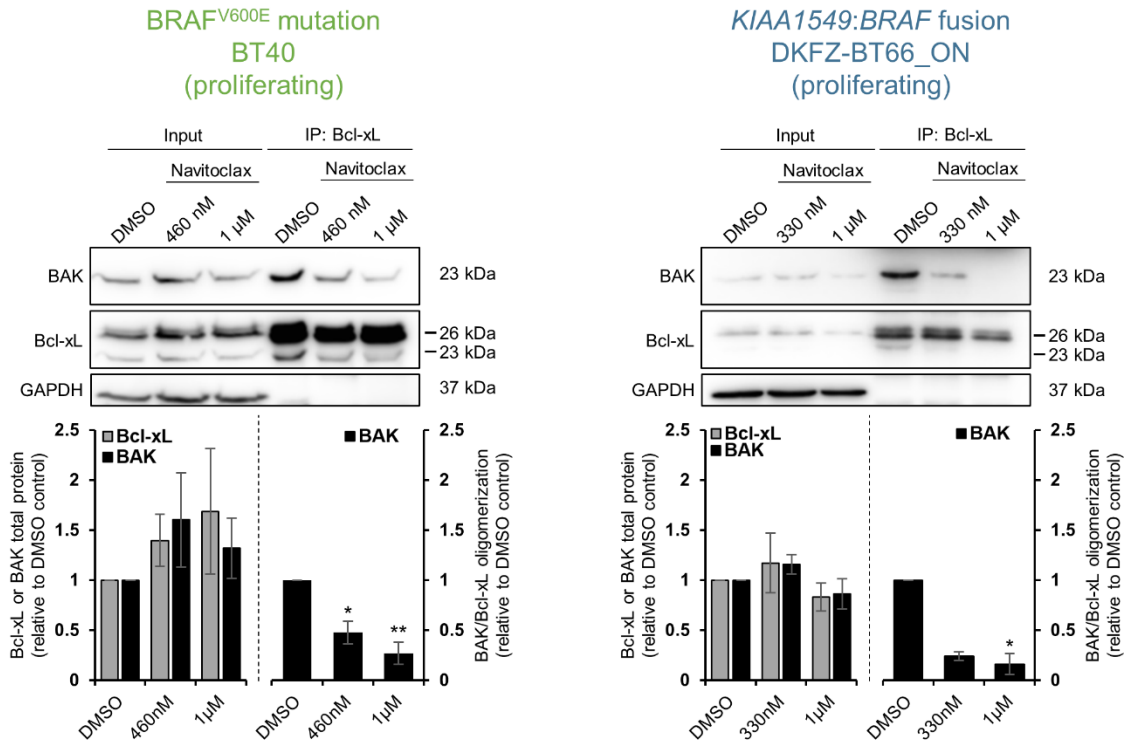


314 **Supplementary Fig. S8: Ulixertinib on-target activity *in vitro* via RPPA**
315 **and Western blot**

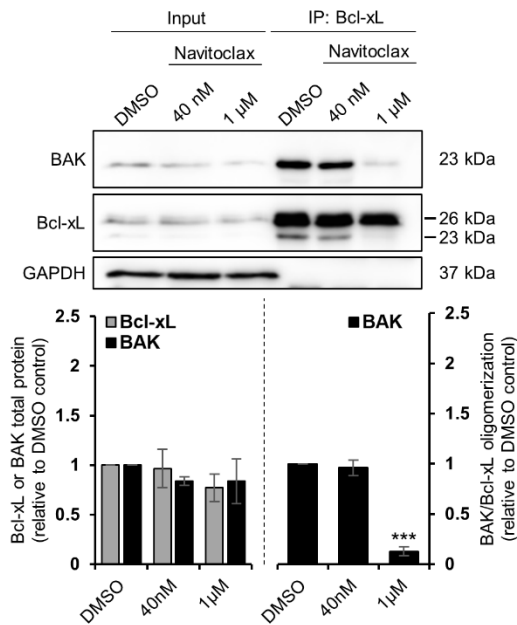
316 A, Heatmap depicting phosphoprotein fold changes of selected markers upon
317 treatment in RPPA. Fold change relative to DMSO is shown, with red colors
318 indicating an increased phosphorylation, and blue colors indicating decreased
319 phosphorylation. Red dotted rectangle (cluster 1) highlights the cluster of samples
320 with an increased phosphorylation upon treatment; blue dotted rectangle (cluster 2)
321 highlights the cluster of samples with a decreased phosphorylation upon treatment.

322 B, C, and D, Western blot analysis of DUSP6 in BT40 (B), DKFZ-BT66_ON (C), and
323 DKFZ-BT66_OFF (D), treated with varying concentrations of ulixertinib (2x IC₅₀,
324 1x IC₅₀, 0.5x IC₅₀) and a fixed concentration (IC₅₀) of the combination partner. Are
325 depicted: quantification (n = 3 biological replicates) of all treatment conditions relative
326 to the DMSO control; individual quantification for each classes of combination
327 partners, depicting DUSP6 quantification relative to DUSP6 levels in the
328 corresponding combination partner single treatment; estimation of the expected effect
329 based on the Bliss independence formula compared to the observed effect. Depicted
330 are data from three biological replicates. Significant differences are indicated as *, P
331 < 0.05; **, P < 0.01; ***, P < 0.001 (ANOVA followed Tukey's honest significant test).

Supplementary Fig. S9



**KIAA1549:BRAF fusion
DKFZ-BT66_OFF
(senescent)**

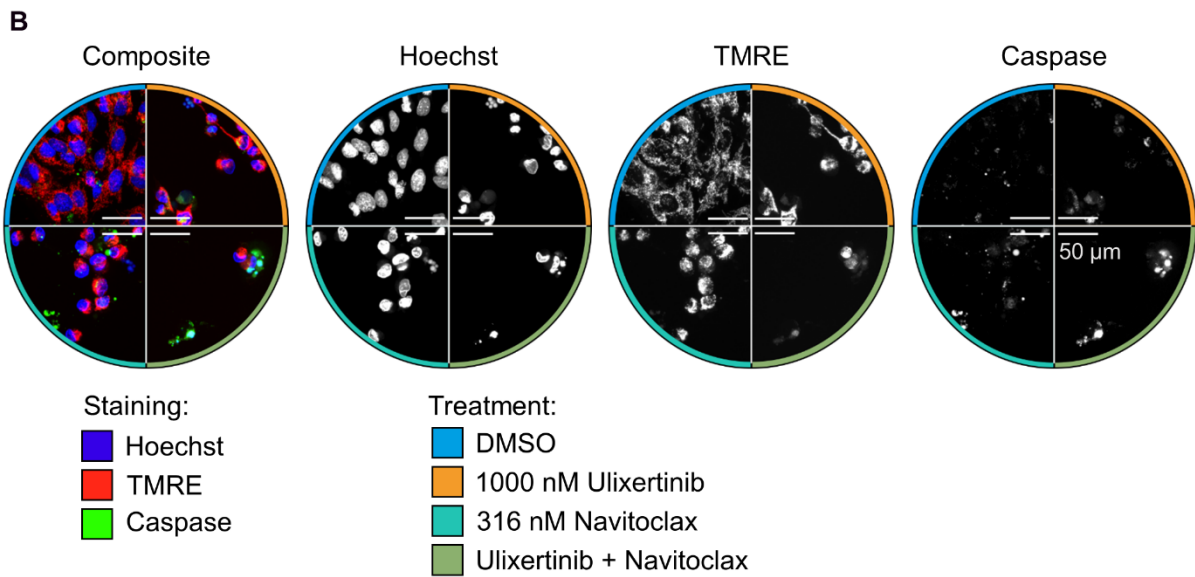
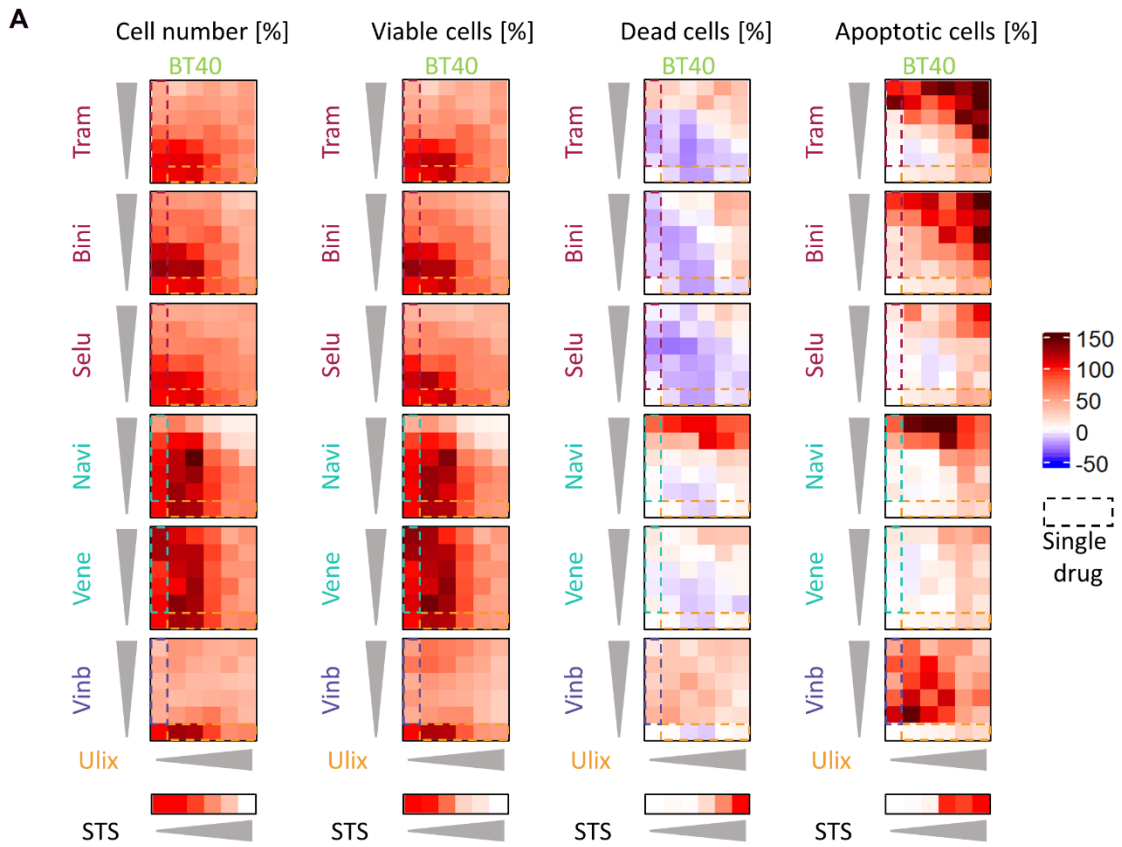


333 **Supplementary Fig. S9: Navitoclax on-target activity *in vitro* via**

334 **immunoprecipitation**

335 BT40, DKFZ-BT66_ON and DKFZ-BT66_OFF cells were treated for 4 h with the
336 corresponding navitoclax IC₅₀, 1 μM navitoclax or DMSO before lysis. Interaction of
337 pro-apoptotic BAK with anti-apoptotic Bcl-xL was assessed by immunoprecipitation
338 with a Bcl-xL specific antibody. Are depicted one representative experiment for each
339 cell line. Is also shown Western blot quantification of 3 independent biological
340 replicates. The left pane shows BAK and Bcl-xL normalized to the loading control
341 GAPDH, and normalized to DMSO. The right pane shows BAK/Bcl-xL ratio, and
342 normalized to DMSO. Significant differences are indicated as *, P < 0.05; **, P <
343 0.01; ***, P < 0.001 (ANOVA followed Tukey's honest significant test).

Supplementary Fig. S10



345 **Supplementary Fig. S10: High content microscope images and analysis**
346 **in BT40 cells**

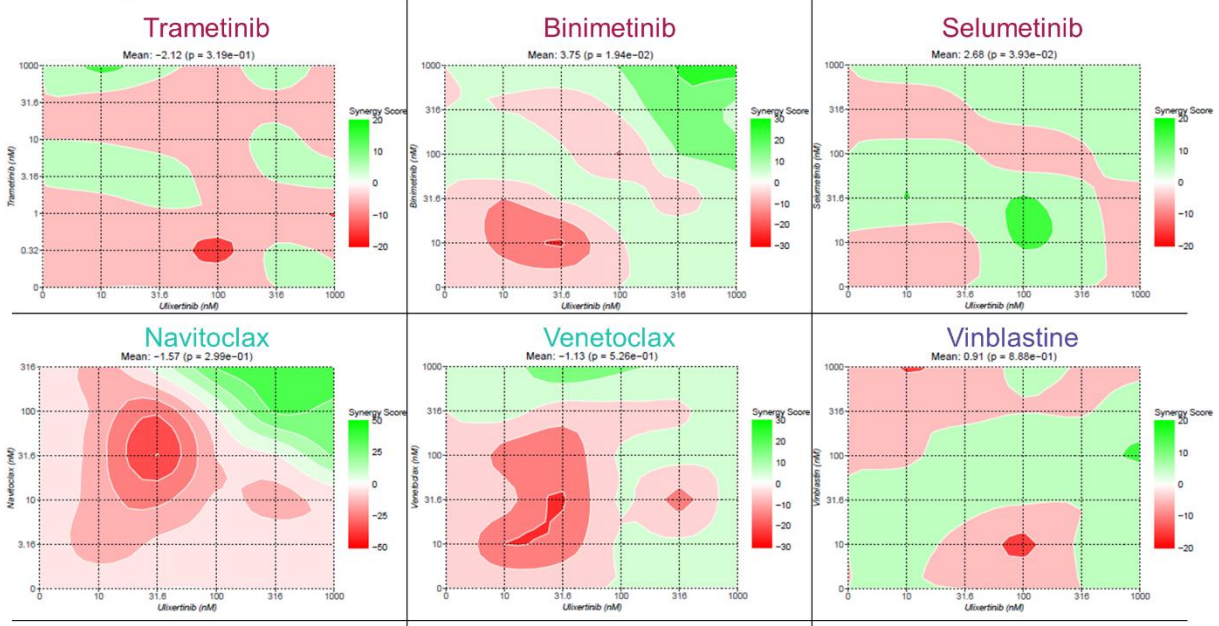
347 A, BT40 cells were treated for 72 h. Each drug was combined using concentration
348 ranges following a 1/2 Log distribution and centered around the corresponding drug's
349 metabolic IC₅₀ rounded to the closest power of 10 (10 nM or 100 nM, as indicated):
350 0, 10, 31.6, 100, 316, 1000 nM ulixertinib (Ulix) alone or in combination with 0, 0.31,
351 1, 3.16, 10, 31.6, 1000 nM trametinib (Tram), 0, 10, 31.6, 100, 316, 1000 nM
352 binimetinib (Bini), 0, 10, 31.6, 100, 316, 1000 nM selumetinib (Selu), 0, 3,16, 10,
353 31.6, 100, 316 nM navitoclax (Navi), 0, 10, 31.6, 100, 316, 1000 nM venetoclax
354 (Vene) or 0, 10, 31.6, 100, 316, 1000 nM vinblastine (Vinb). A staurosporine (STS)
355 concentration curve (0, 0.1, 1, 10, 100, 1000 nM) was added as death control. The
356 following readouts were evaluated: percent cell number, percent viable cells, percent
357 dead cells (evaluated by fragmented nuclei) and percent apoptotic cells. All BT40
358 readouts are normalized to DMSO and 1000 nM STS. B, BT40 cells were treated
359 with DMSO, 1000 nM ulixertinib, 316 nM navitoclax and their combination for 72 h.
360 Treatments are indicated by the colored border. The cells were stained with
361 Hoechst33342 (blue), TMRE (red), and CellEvent Caspase3/7 stain (green). The
362 scale bar represents 50 µm. Depicted are data from at least three biological
363 replicates.

364

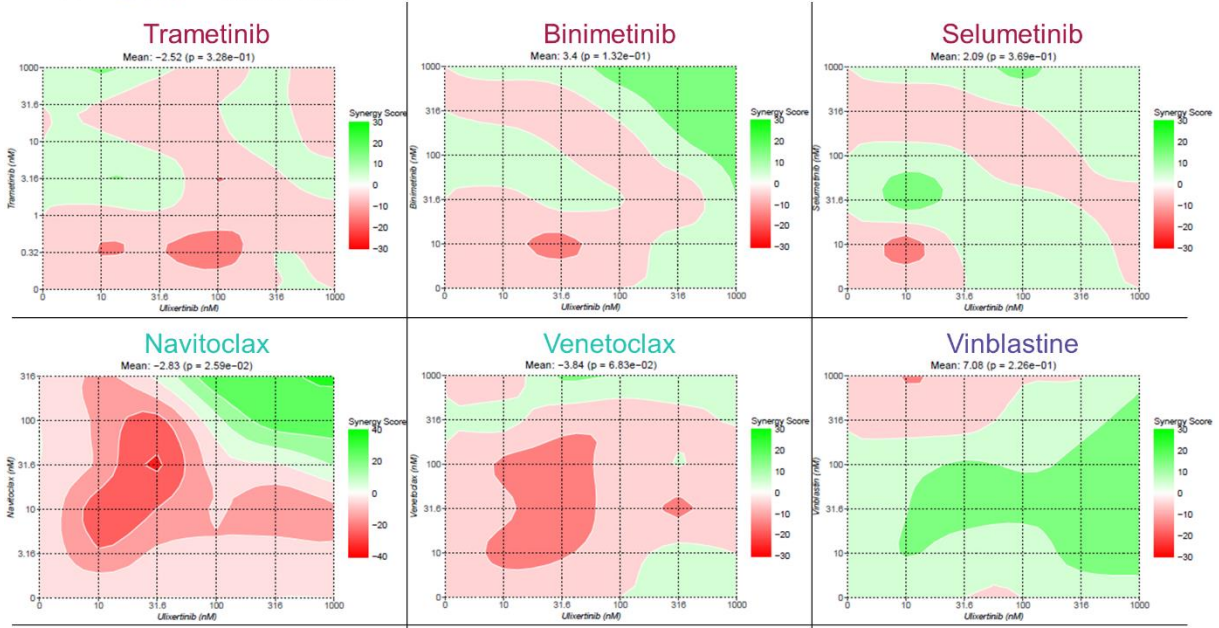
365

Supplementary Fig. S11

A - BT40 – Cell number

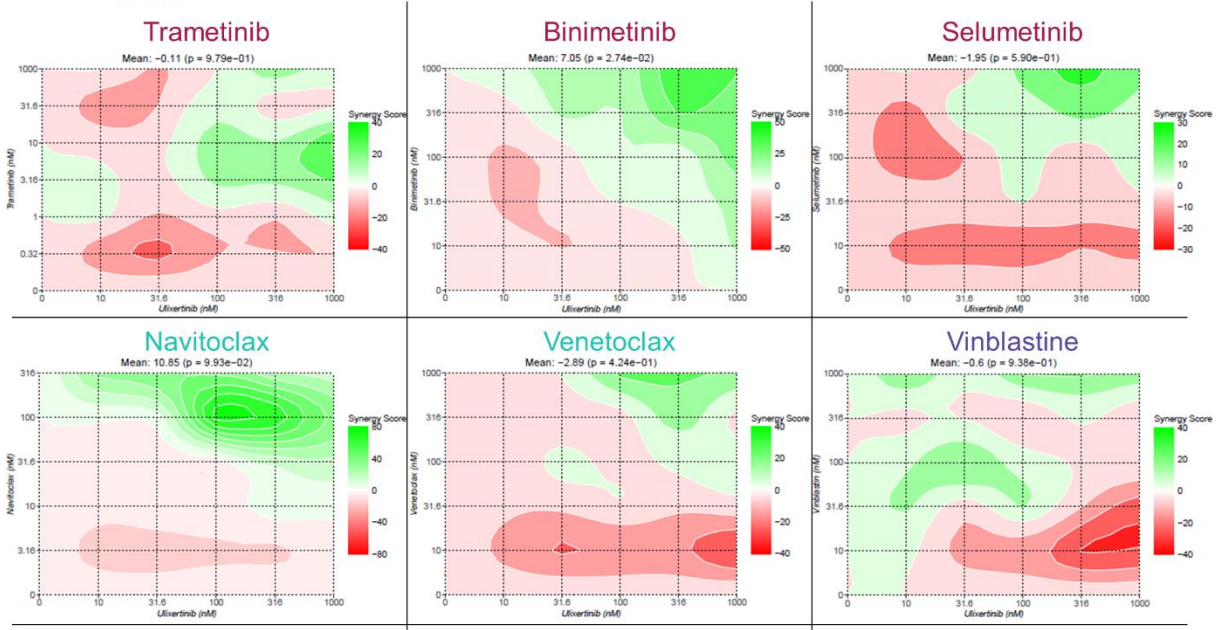


B - BT40 – Viable cells

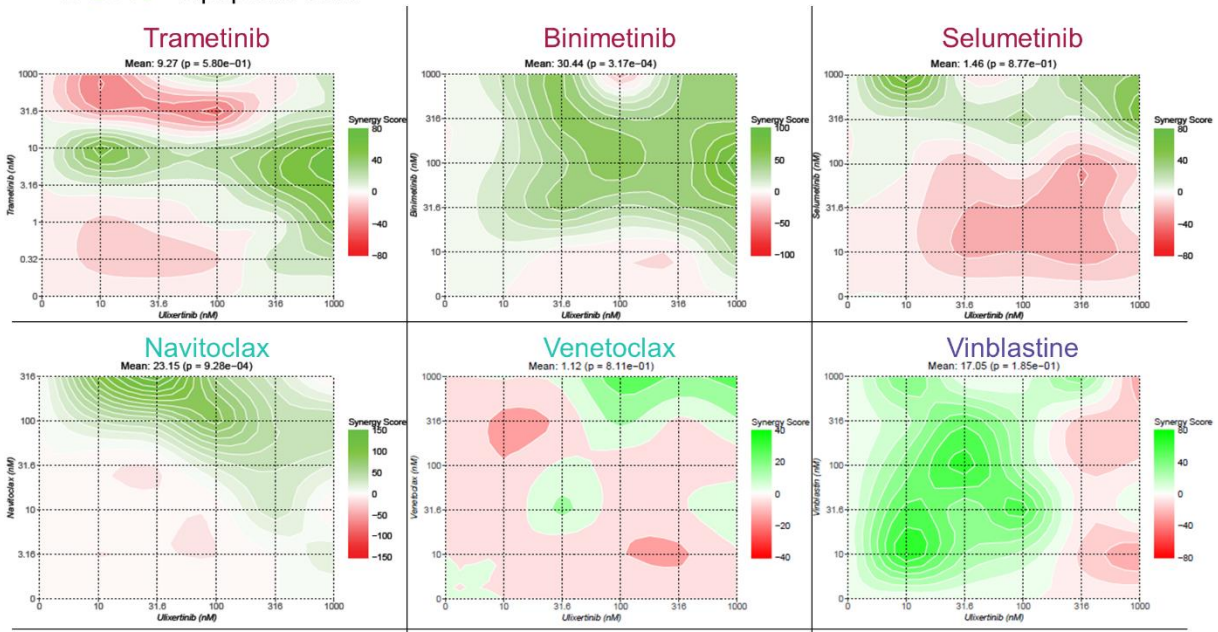


Supplementary Fig. S11

C - BT40 – Dead cells



D-BT40 – Apoptotic cells



367

368 **Supplementary Fig. S11: Synergy analysis of high content microscopy**

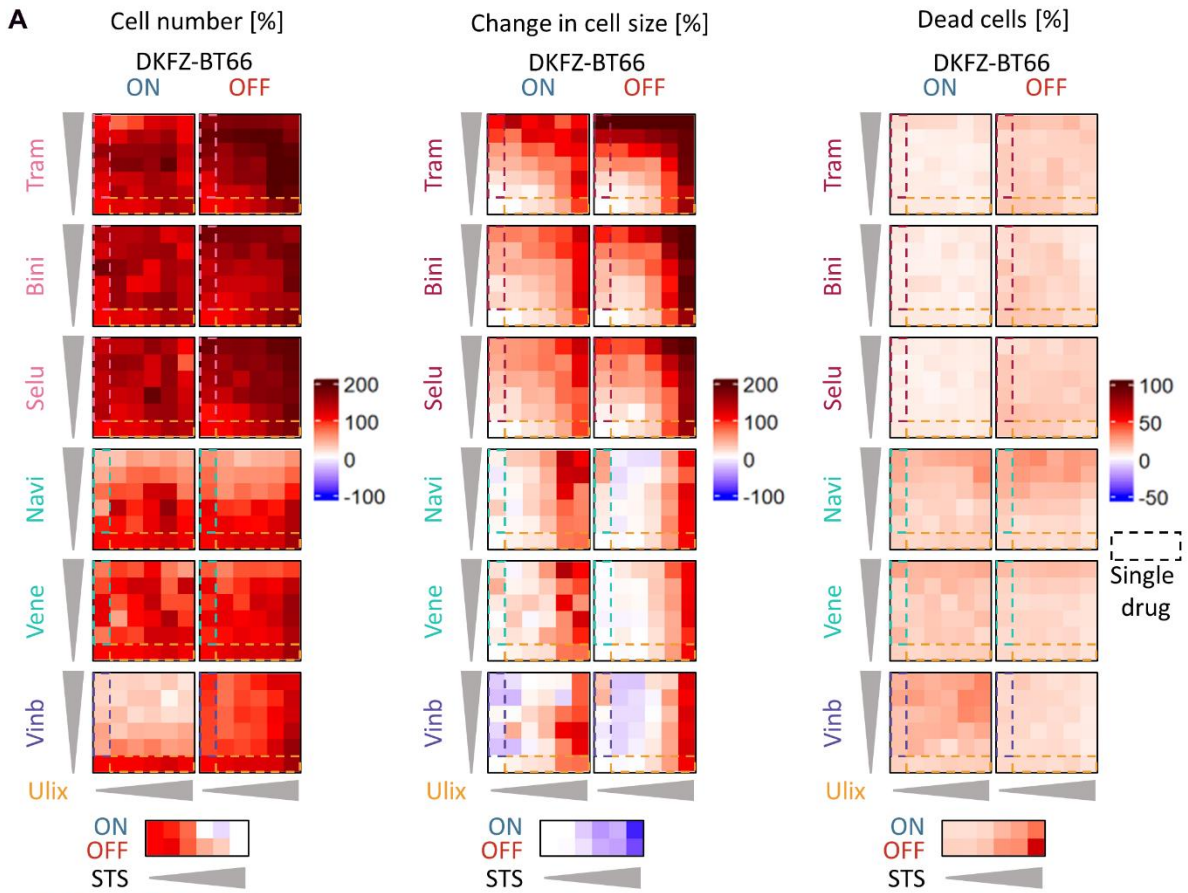
369 **data in BT40 cells**

370 Synergy analysis was calculated with www.synergyfinder.org using the data

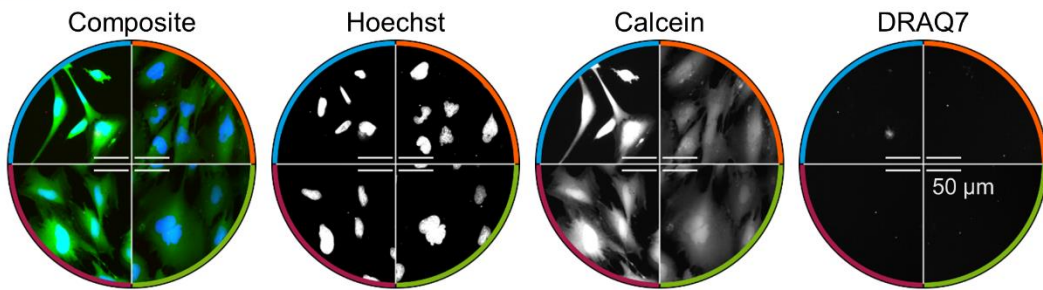
371 presented in Supplementary Fig. S10A. Synergy models used are described in the

372 methods section. The following readouts were evaluated: (A) Cell number, (B) viable
373 cells, (C) dead cells (evaluated by fragmented nuclei), and (D) apoptotic cells.

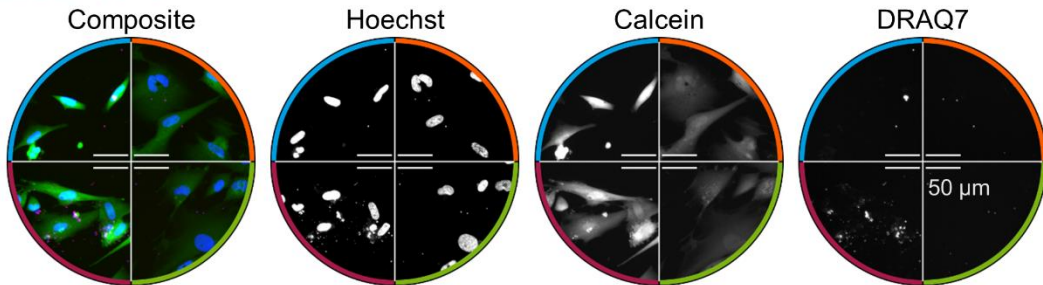
Supplementary Fig. S12



B-DKFZ-BT66-ON



C-DKFZ-BT66-OFF



Staining:
 Hoechst DRAQ7
 Calcein

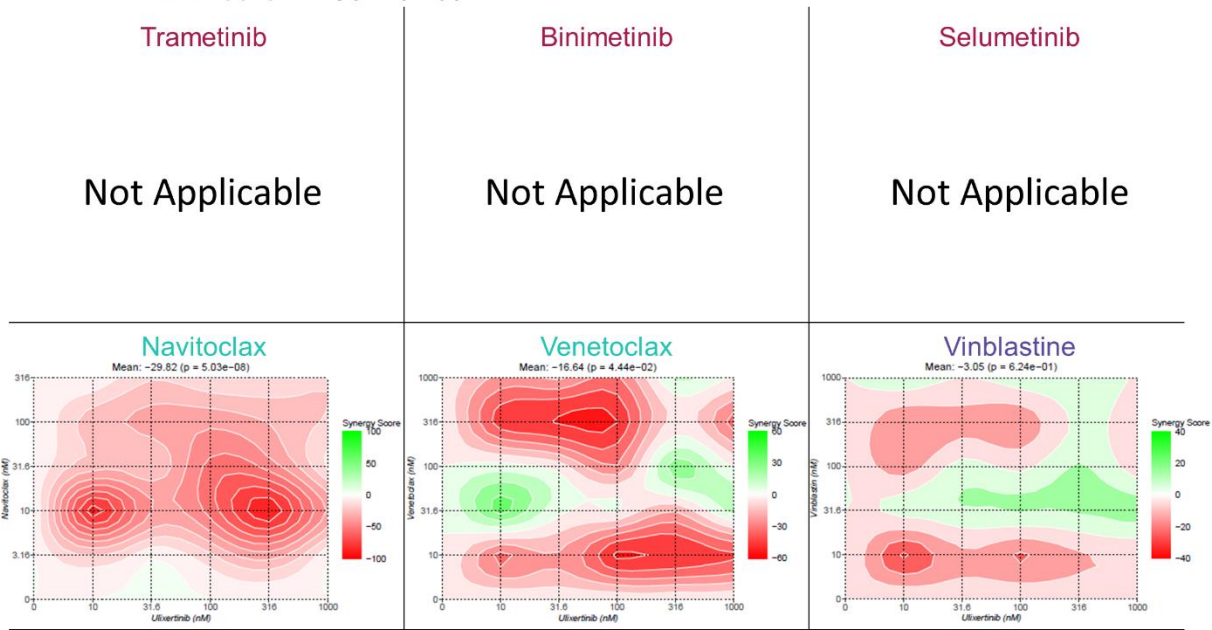
Treatment:
 DMSO 1000 nM Binimetinib
 1000 nM Ulixertinib Ulixertinib + Binimetinib

375 **Supplementary Fig. S12: High content microscope images and analysis**
376 **in DKFZ-BT66 cells**

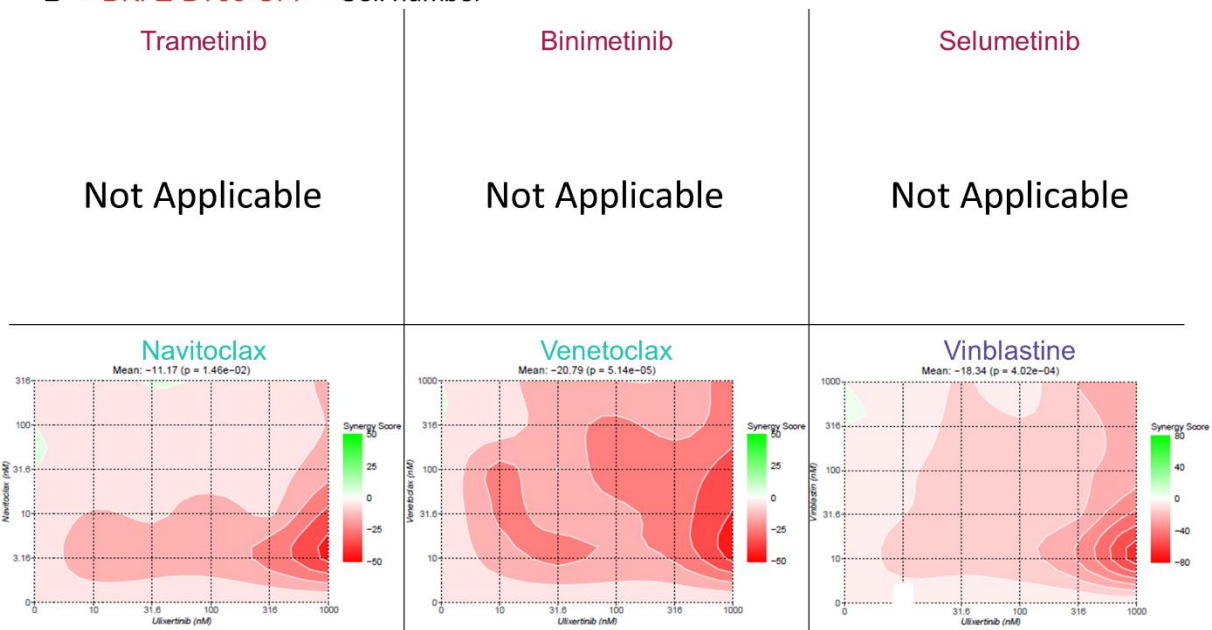
377 A, DKFZ-BT66_ON and DKFZ-BT66_OFF cells were treated for 72 h. Each drug was
378 combined using concentration ranges following a 1/2 Log distribution and centered
379 around the corresponding drug's metabolic IC₅₀ rounded to the closest power of 10
380 (10 nM or 100 nM, as indicated): 0, 10, 31.6, 100, 316, 1000 nM ulixertinib (Ulix)
381 alone or in combination with 0, 0.31, 1, 3.16, 10, 31.6, 1000 nM trametinib (Tram), 0,
382 10, 31.6, 100, 316, 1000 nM binimetinib (Bini), 0, 10, 31.6, 100, 316, 1000 nM
383 selumetinib (Selu), 0, 3,16, 10, 31.6, 100, 316 nM navitoclax (Navi), 0, 10, 31.6, 100,
384 316, 1000 nM venetoclax (Vene) or 0, 10, 31.6, 100, 316, 1000 nM vinblastine
385 (Vinb). A staurosporine (STS) concentration curve (0, 0.1, 1, 10, 100, 1000 nM) was
386 added as death control. For DKFZ-BT66 the readouts used were in percent: cell
387 number (normalized to DMSO and 1000 nM staurosporine), change in cell size
388 (normalized to DMSO), and dead cells (evaluated as percent of DRAQ7 positive
389 nuclei). B-C, DKFZ-BT66 were treated for with DMSO, 1000 nM ulixertinib, 1000 nM
390 binimetinib, and their combination for 72 h. Treatments are indicated by the colored
391 border. The cells were stained with Hoechst33342 (blue), calceinAM (green), and
392 DRAQ7 (red). The scale bar represents 50 µm. Depicted are data from at least three
393 biological replicates.

Supplementary Fig. S13

A - DKFZ-BT66-ON – Cell number

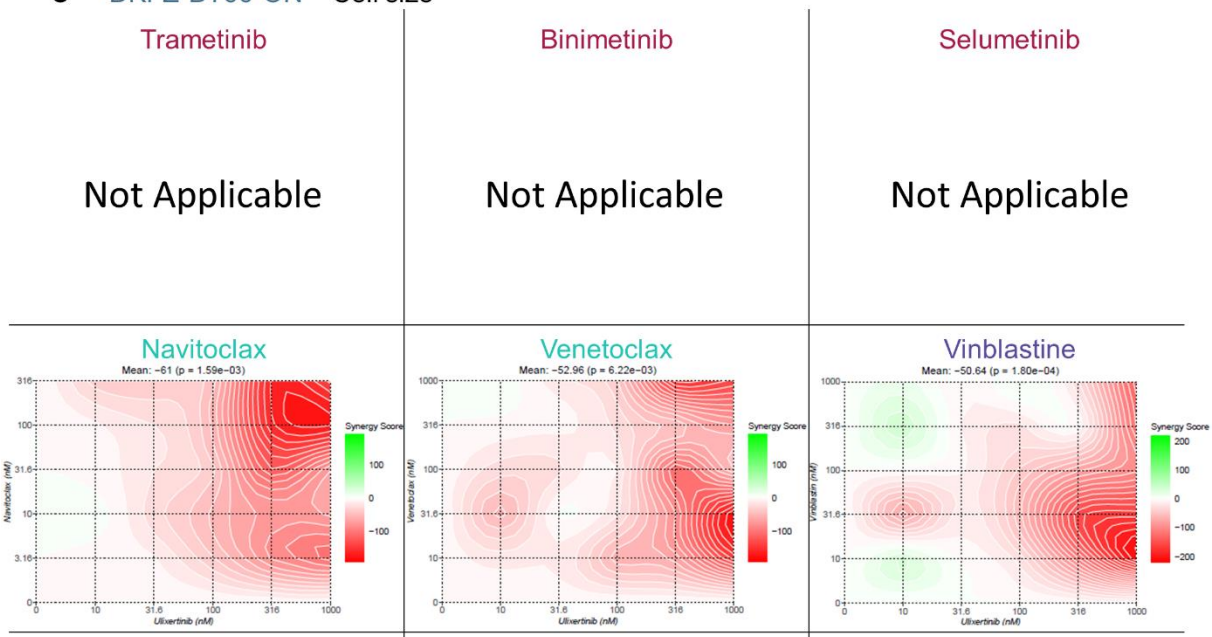


B - DKFZ-BT66-OFF – Cell number

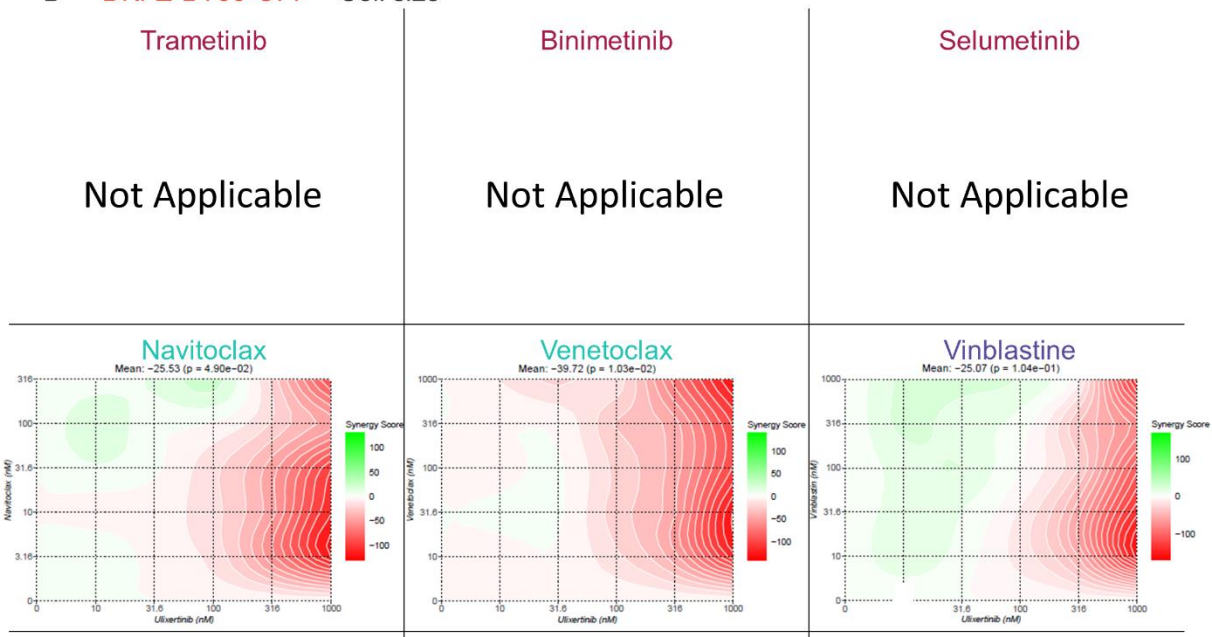


Supplementary Fig. S13

C - DKFZ-BT66-ON – Cell size

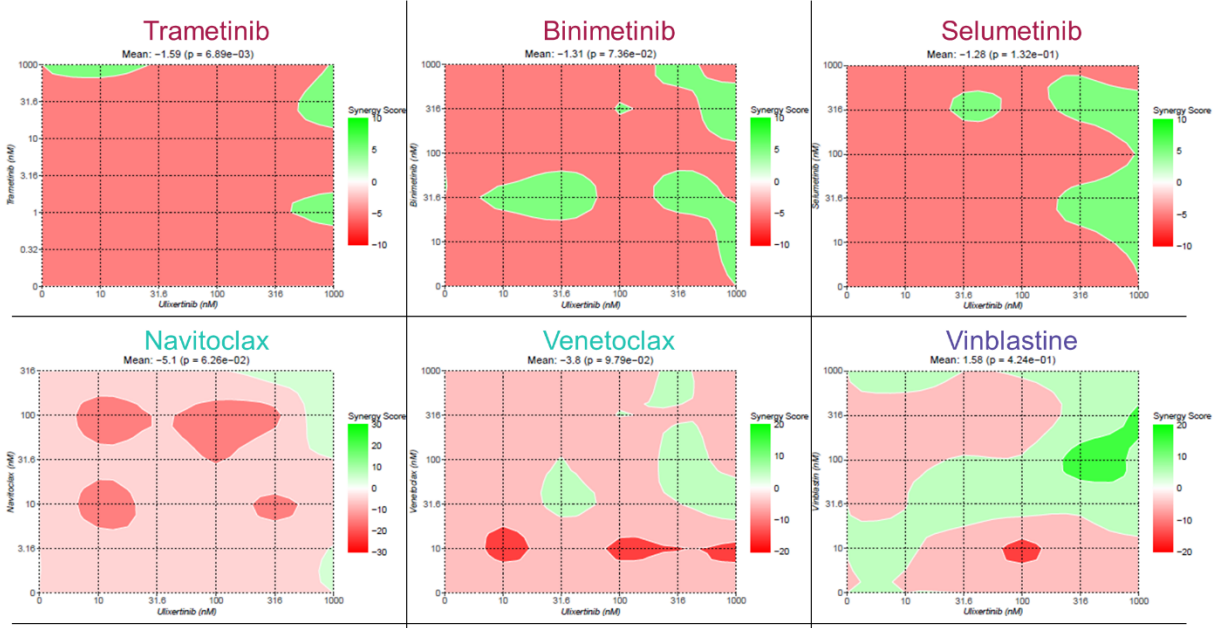


D - DKFZ-BT66-OFF – Cell size

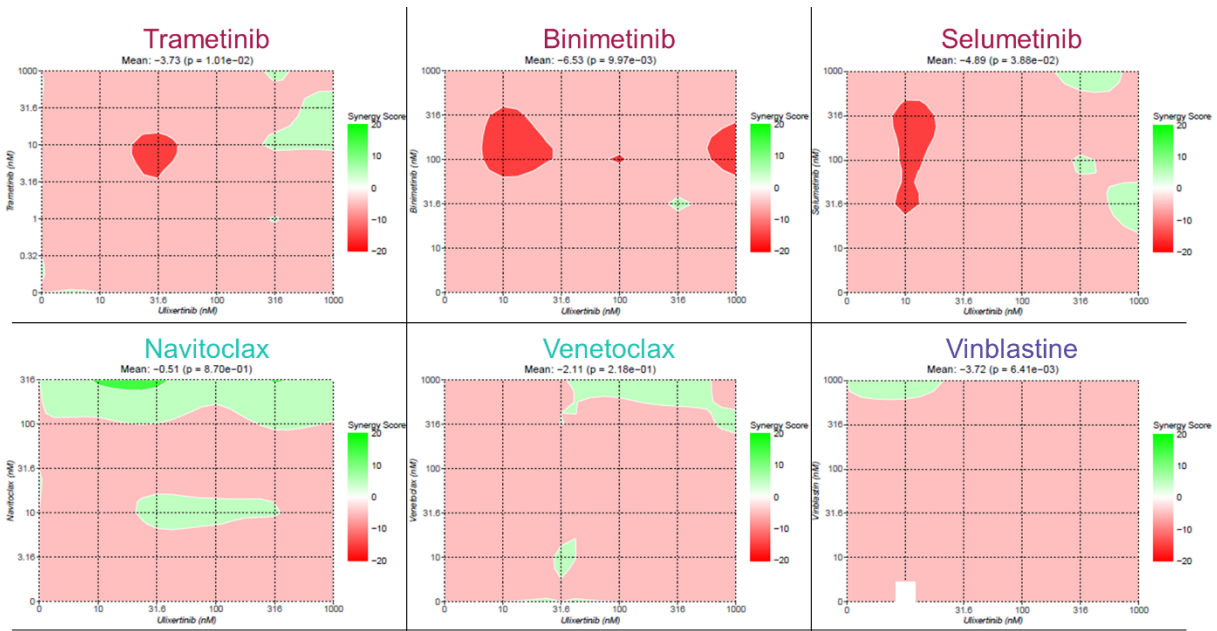


Supplementary Fig. S13

E - DKFZ-BT66-ON – Dead cells



F - DKFZ-BT66-OFF – Dead cells



396

397 **Supplementary Fig. S13: Synergy analysis of high content microscopy**

398 **data in DKFZ-BT66 cells**

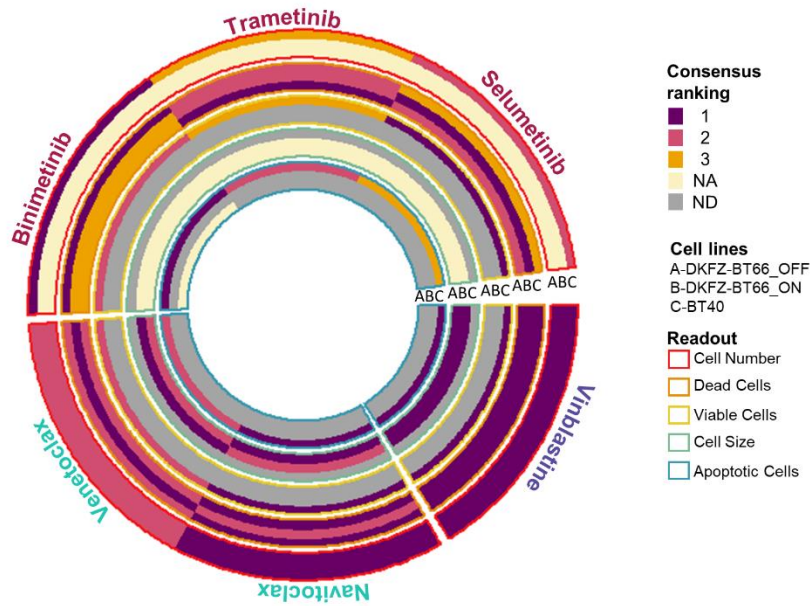
399 Synergy analysis was calculated with www.synergyfinder.org using the data

400 presented in Supplementary Fig. S12A. Synergy models used are described in the

401 methods section. The readouts used were: (A-B) cell number, (C-D) change in cell

402 size, and (E-F) dead cells (evaluated as percent of DRAQ7 positive nuclei). Synergy
403 scores for cell number and cell size could not be calculated for trametinib,
404 binimetinib, and selumetinib in both DKFZ-BT66 cell lines.

Supplementary Fig. S14

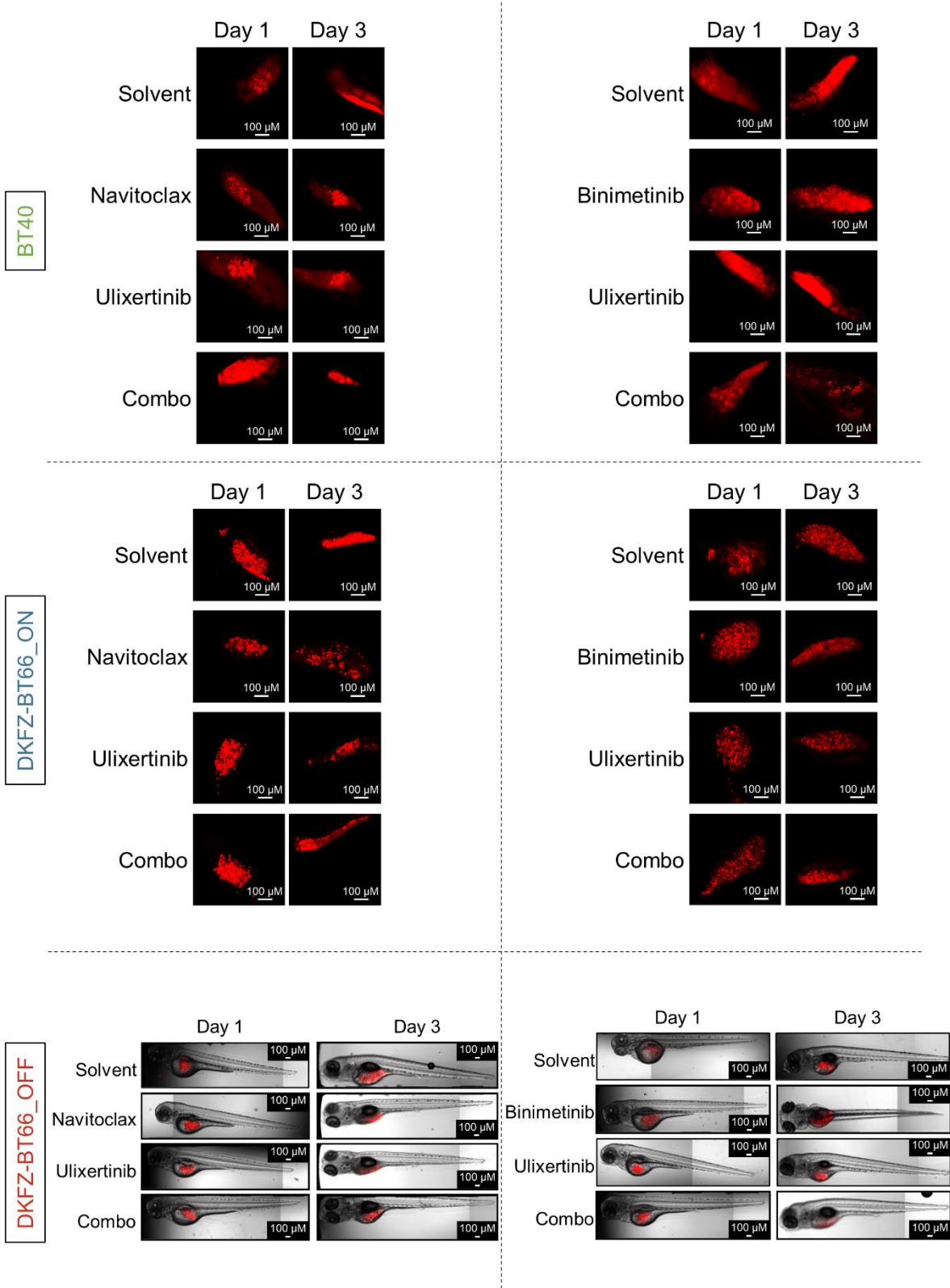


405

406 **Supplementary Fig. S14: Consensus ranking of combination partners in**
 407 **the high content microscopy *in vitro* screen**

408 Circular heatmap summarizing the individual drug's performance per drug class,
 409 following consensus ranking across synergy metrics. The ranking was calculated for
 410 the DKFZ-BT66_OFF, DKFZ-BT66_ON, and BT40 models (respectively designated
 411 by A, B, and C) and for each HCM readout (from outermost rings to innermost rings:
 412 cell number, dead cells, viable cells, cell size, and apoptotic cells).

Supplementary Fig. S15



414 **Supplementary Fig. S15: pLGG cell lines transplantation in zebrafish**

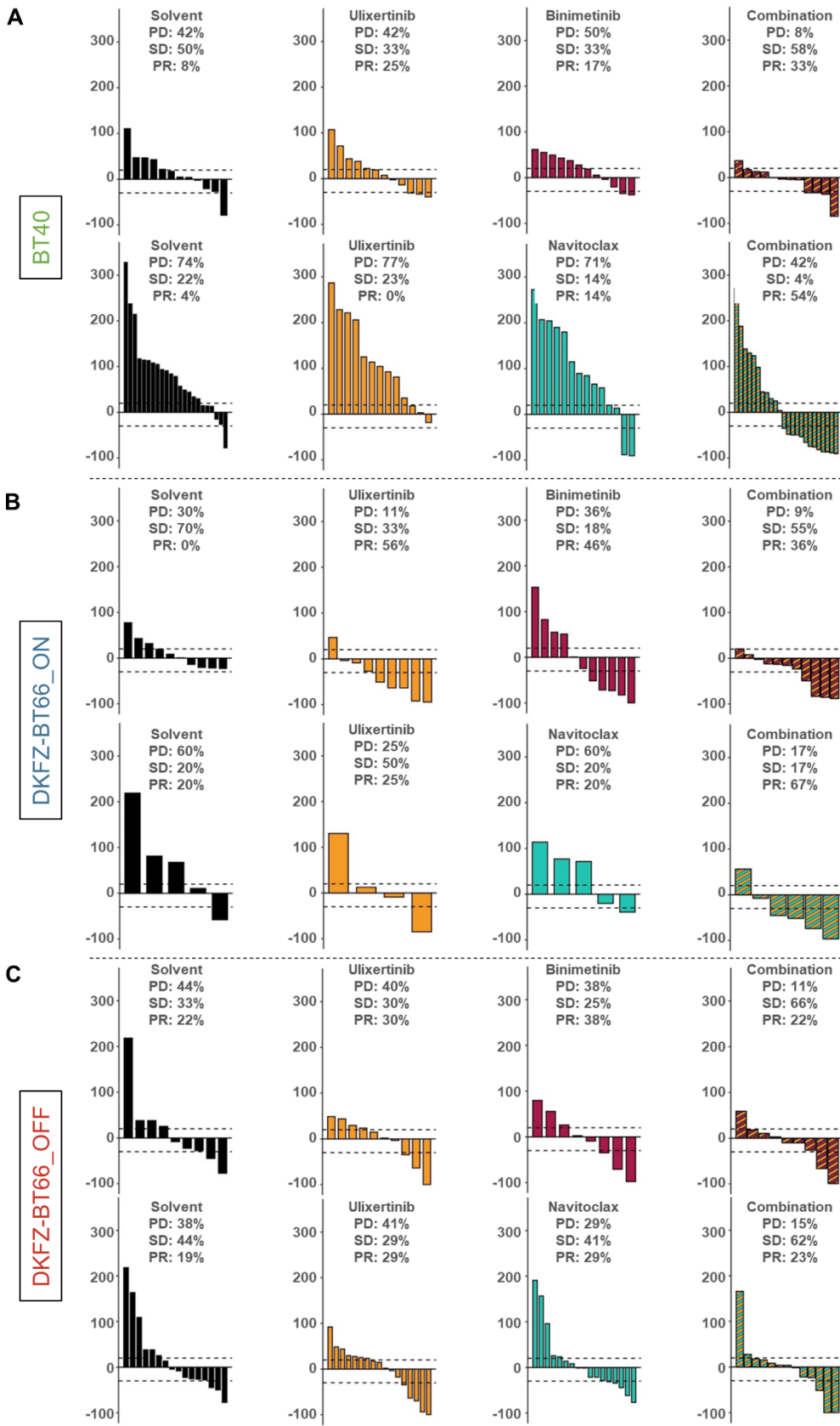
415 **embryo *in vivo***

416 Exemplary pictures of pLGG cell line transplantation in zebrafish embryos. Are shown
417 picture from one representative embryo transplanted with BT40, BT66_ON, or DKFZ-
418 BT66_OFF, after 1 day (baseline) and 3 days (endpoint) of treatment as indicated.

419 The scale bar represents 100 μm .

420

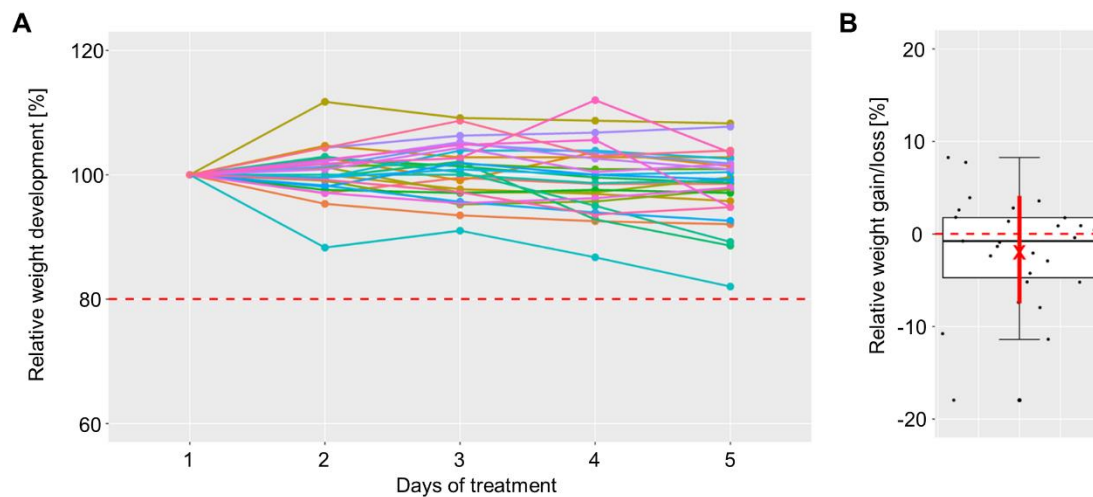
Supplementary Fig. S16



422 **Supplementary Fig. S16: Zebrafish embryo validation of ulixertinib's**
423 **combination partners**

424 Waterfall plots showing the change from baseline (in %) for tumor volume upon
425 treatment for each individual tested zebrafish embryo with A) BT40, (B) DKFZ-
426 BT66_ON, or (C) DKFZ-BT66_OFF xenografts. Drugs were applied to the embryo-
427 surrounding buffer solution in the following concentrations: ulixertinib (1 μ M),
428 binimetinib (2 μ M), and navitoclax (5 μ M). PD, progressive disease; SD, stable
429 disease; PR, partial response. n= 4 – 23 embryos/group.

430

Supplementary Fig. S17

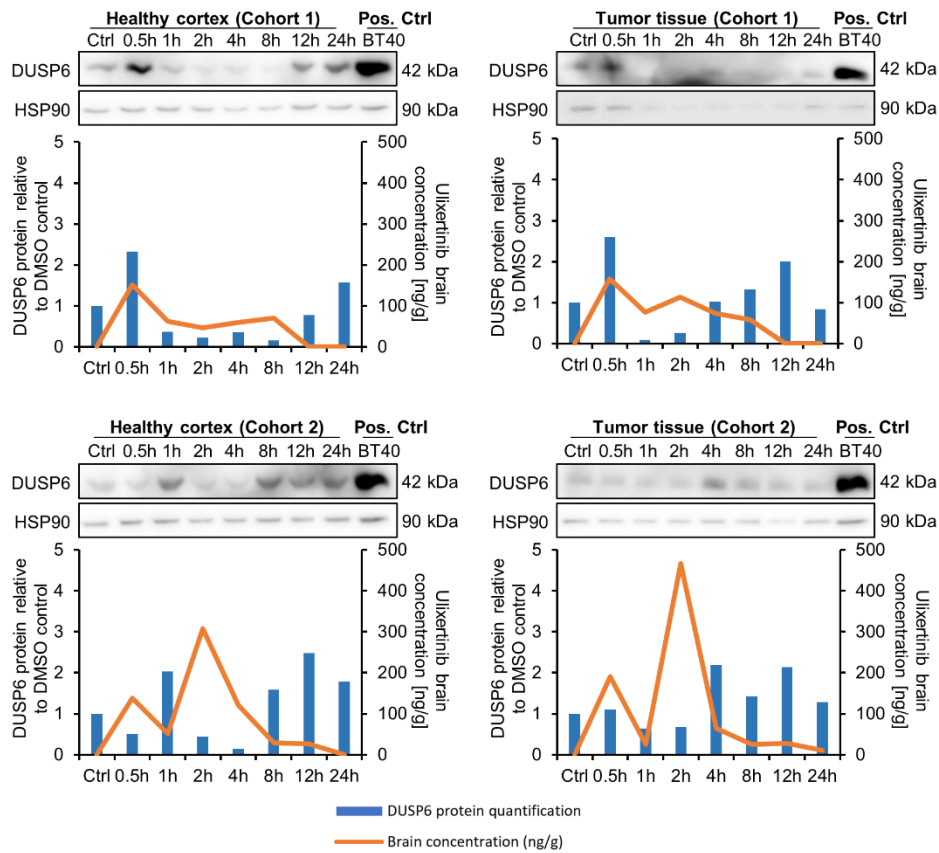
431

432 **Supplementary Fig. S17: Relative weight development as surrogate for in**
433 **vivo toxicity during ulixertinib treatment in the pharmacokinetic study.**

434 A, BT40-PDX mice were treated with ulixertinib (p.o. 80 mg/kg, 2x/day for five days,
435 n=28) and relative weight development was monitored for the treatment period.

436 Different colors represent individual mice. Exclusion criterion of a maximal weight
437 loss of 20% is indicated as red line. B, Relative weight development was plotted after
438 calculating the average difference of animal's weight before the dosing and at the
439 end of treatment. Initial weight is indicated by the red dashed line. Mean (red cross) \pm
440 S.D. (red line) are highlighted.

Supplementary Fig. S18



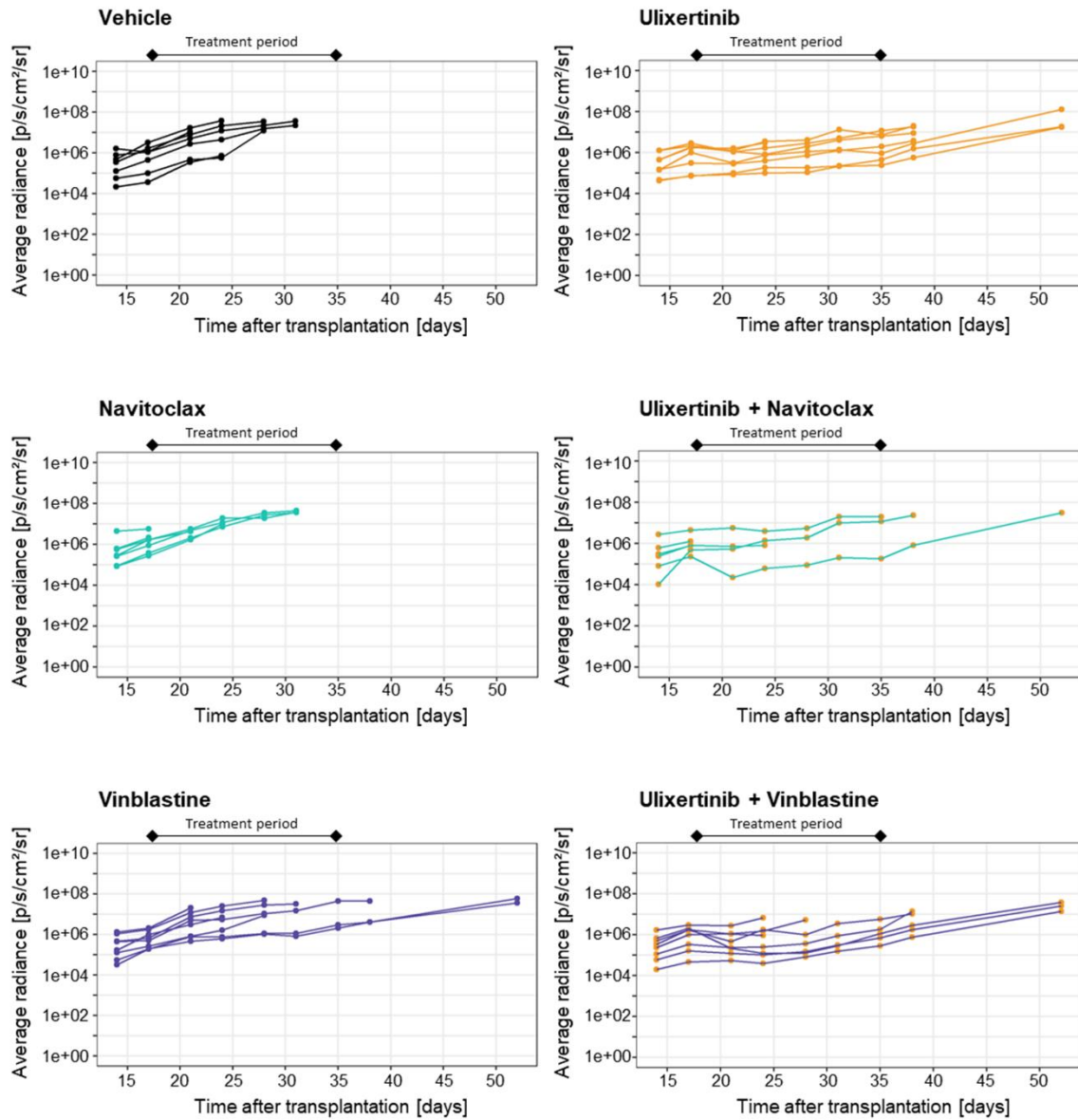
441

442 **Supplementary Fig. S18: Ulixertinib on-target activity in vivo.**

443 Western blot analysis of the DUSP6 and HSP90 proteins in tissue samples from both
 444 cohorts and both tissues (healthy and tumor). Depicted blots represent data from a
 445 single mouse per time point. Western blot quantification is shown (blue bars),
 446 depicting DUSP6 signal normalized to its corresponding HSP90, and normalized to
 447 the DMSO control.

448

Supplementary Fig. S19

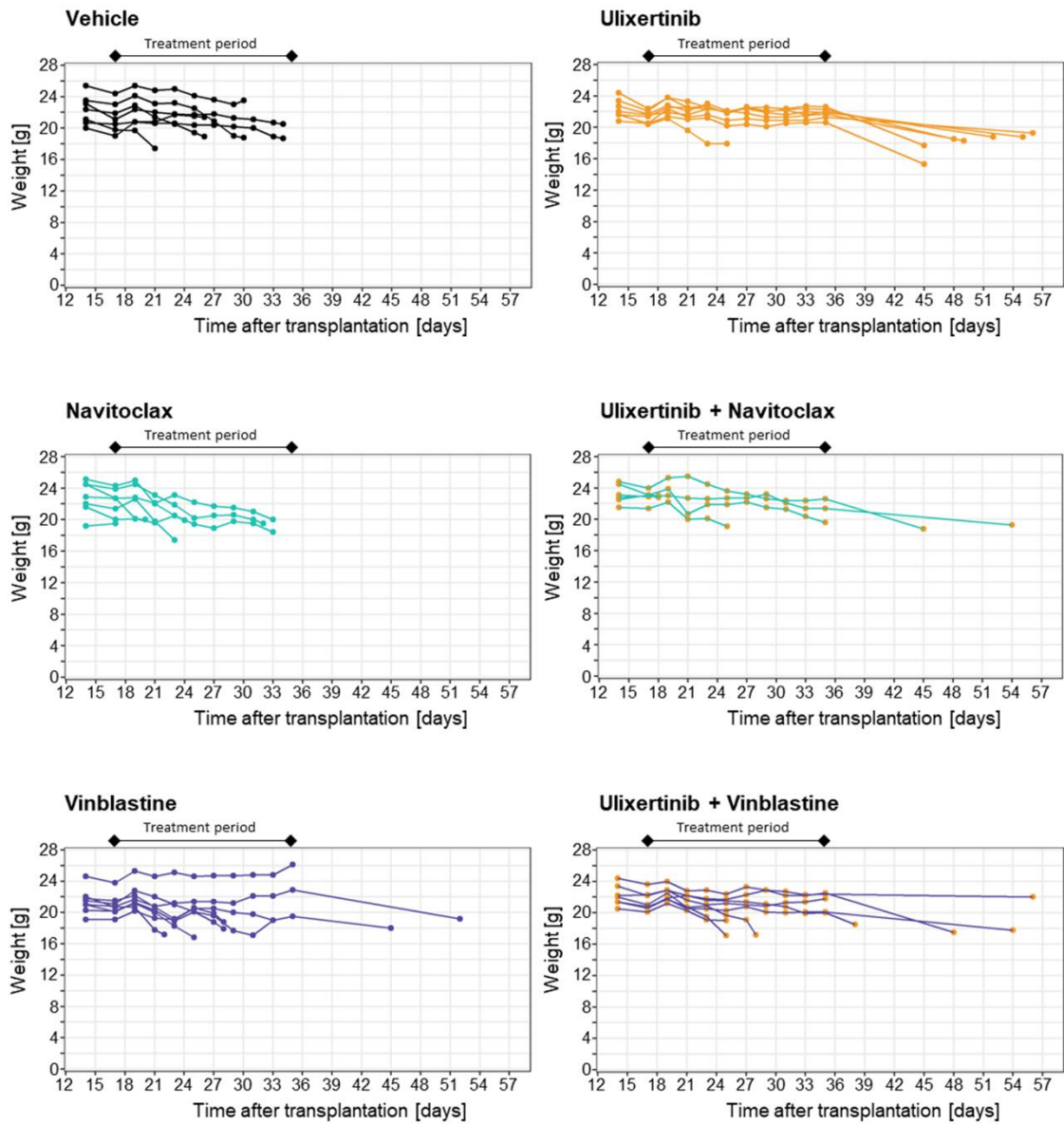


449

450 **Supplementary Fig. S19: Bioluminescence signals representing tumor**
 451 **volumes in PDX mice**

452 Tumor volumes according to bioluminescence measurements from individual animals
 453 during treatments as indicated (n=8 mice per group). Luciferase signal were
 454 measured in photons/sec/cm²/steradian over the entire treatment- and observation-
 455 period. Ultimately censored animals are not depicted.

Supplementary Fig. S20



456

457 **Supplementary Fig. S20: Mouse weight development during the**
458 **preclinical *in vivo* study**

459 Weights of animals clustered by treatment as indicated (n=8 mice per group).

460 Ultimately censored animals are not depicted.

Supplementary Fig. S21

	BT40		DKFZ-BT66-ON		DKFZ-BT66-OFF		
	Matrix	Ray	Matrix	Ray	Matrix	Ray	
	Ulixertinib	Ulixertinib	Ulixertinib	Ulixertinib	Ulixertinib	Ulixertinib	
Trametinib							Metabolic activity
Binimetinib							
Selumetinib							
A-1331852							
Navitoclax							
Venetoclax							
Vinblastine							
Carboplatin							
Trametinib							MAPK reporter assay
Binimetinib							
Selumetinib							
A-1331852							
Navitoclax							
Venetoclax							
Vinblastine							
Carboplatin							
Trametinib							Cell number
Binimetinib							
Selumetinib							
A-1331852							
Navitoclax							
Venetoclax							
Vinblastine							
Carboplatin							
Trametinib							Viable cells
Binimetinib							
Selumetinib							
A-1331852							
Navitoclax							
Venetoclax							
Vinblastine							
Carboplatin							
Trametinib							Dead cells
Binimetinib							
Selumetinib							
A-1331852							
Navitoclax							
Venetoclax							
Vinblastine							
Carboplatin							
Trametinib							Apoptotic cells
Binimetinib							
Selumetinib							
A-1331852							
Navitoclax							
Venetoclax							
Vinblastine							
Carboplatin							
Trametinib							Cell size
Binimetinib							
Selumetinib							
A-1331852							
Navitoclax							
Venetoclax							
Vinblastine							
Carboplatin							

Synergy models
■ Loewe
■ Bliss
■ HSA
■ NA
■ ND

462 **Supplementary Fig. S21: Summary of the synergy models used *in vitro***

463 Summary of all synergy models (Loewe, Bliss, Highest single agent HSA) used per
464 cell line, per combination, per readout, in the *in vitro* screen and in the high content
465 microscopy validation. NA, not applicable due to readout inconsistency. ND, not
466 determined.

467

468 **Supplementary Tables**469 **Supplementary Table S1: Seeding densities for in vitro assays**

Cell line	Experiment type	Plate type	Seeding densities (cells/well)
BT40	Metabolic activity measurement	384-well	300
DKFZ-BT66_ON	Metabolic activity measurement	384-well	300
DKFZ-BT66_OFF	Metabolic activity measurement	384-well	4 800
BT40-pDIPZ	MAPK reporter activity measurement	384-well	3 000
DKFZ-BT66_ON-pDIPZ	MAPK reporter activity measurement	384-well	1 500
DKFZ-BT66_OFF-pDIPZ	MAPK reporter activity measurement	384-well	6 000
BT40	High-content microscopy measurements	384-well	500
DKFZ-BT66_ON	High-content microscopy measurements	384-well	1 000
DKFZ-BT66_OFF	High-content microscopy measurements	384-well	8 000
BT40	On-target activity measurement (WB/RPPA)	6-well	500 000
DKFZ-BT66_ON	On-target activity measurement (WB/RPPA)	6-well	500 000
DKFZ-BT66_OFF	On-target activity measurement (WB/RPPA)	6-well	1 000 000
BT40	On-target activity measurement (IP)	10 cm dish	5 000 000
DKFZ-BT66_ON	On-target activity measurement (IP)	10 cm dish	3 000 000
DKFZ-BT66_OFF	On-target activity measurement (IP)	10 cm dish	5 000 000

470

471

472 **Supplementary Table S2: Markers conditions for high content**473 **microscopy analysis**

Cell line	Marker	Supplier	Cat. No.	Concentration
BT40	Hoechst33342	ThermoFisher Scientific	H3570	10 µg/ml
BT40	TMRE	Abcam	ab113852	1 µM
BT40	CellEvent Caspase3/7	ThermoFisher Scientific	C10723	8 µM
DKFZ-BT66	Hoechst33342	ThermoFisher Scientific	H3570	10 µg/ml
DKFZ-BT66	CalceinAM	ThermoFisher Scientific	65-0853-39	1.25 µM
DKFZ-BT66	DRAQ7	ThermoFisher Scientific	D15106	0.6 µM

474

475

476 **Supplementary Table S3: In vitro synergy screens datasets**

477 (See Excel file)

478 **Supplementary Table S4: Antibodies used for WB, IP and RPPA analyses**

Antibody	Species	Clonality	Supplier	Cat. No.	Dilution	Application
DUSP6	Rabbit	Poly-clonal	Cell Signaling	50945	1:1000	<i>In vitro</i> validation
DUSP6	Mouse	Mono-clonal	Santa Cruz	sc-377070	1:1000	<i>In vivo</i> validation
GAPDH	Mouse	Mono-clonal	Merck	MAB374	1:1000	<i>In vitro & in vivo</i> validation
BCL-XL	Rabbit	Mono-clonal	Abcam	ab32370	5µg	Immuno-precipitation
BAK	Rabbit	Mono-clonal	Abcam	ab32371	1:1000	Immuno-precipitation

479

480

481 **Supplementary Table S5: Antibodies used for RPPA and RPPA analyses**

Protein name	MW (kDa)	Function	Cascade position
MEK1/2 S217.S221	45	MEK1/2 is activated by a wide variety of growth factors and cytokines and also by membrane depolarization and calcium influx *S298 phosphorylated by PAK1, facilitates signal transduction from Raf to MEK1 and Erk2 *T386 ERK-mediated phosphorylation, interferes with PAK phosphorylation of MEK1 *S217/S221 phosphorylation and activation by RAF	Upstream activator
ERK1/2 T202.Y204	42, 44	Kinases involved in proliferation, differentiation, motility, and death => phosphorylated and activated by MEK1/1	Target
p90RSK T359.S363	90	Widely expressed Ser/Thr kinases, activated by MAPK pathway *T359/S363 phosphorylated by ERK1/2 and ERK5	Cytosolic target
p90RSK S380	90	Widely expressed Ser/Thr kinases, activated by MAPK pathway *S380 docking site for the constitutively active Ser/Thr kinase PDK1, which in turn phosphorylates p90RSK at Ser221 within the N-terminal kinase domain activation loop, resulting in full enzymatic activation of p90RSK	Cytosolic target
RSK3 T356.S360	90	Widely expressed Ser/Thr kinases, activated by MAPK pathway	Cytosolic target
STAT3 Y705	79,86	Signaling molecule for many cytokines and growth factor receptors; activated in a number of human tumors and possesses oncogenic potential and anti-apoptotic activities *Y727 regulates transcriptional activity through MAPK or mTOR pathways	Cytosolic target
Bim S69	26	Pro-apoptotic protein belonging to the BH3-only group of Bcl-2 family; induces apoptosis by binding to and antagonizing anti-apoptotic members of the Bcl-2 family	Cytosolic target
MSK1 S360	90	Mitogen and stress activated protein kinase => phosphorylation and activation by Erk, p38 MAPK in response to growth factors and cellular stress, respectively	Nuclear target
Elk-1 S383	62	Transcription factor => direct target of the MAPK pathway, phosphorylated and activated by ERK1/2	Nuclear target

CREB S133	43	Transcription factor that activates target genes through cAMP response elements, promoting neuronal survival, precursor proliferation, neurite outgrowth, and neuronal differentiation => phosphorylated and activated by Erk, p90RSK, MSK, CaMKIV, and MAPKAPK-2	Nuclear target
c-Myc S62	62	Transcriptional regulators; proliferation, differentiation and apoptosis => Phosphorylation controls proteasomal-dependent degradation. Mitogens, mitosis, or cellular stress induce phosphorylation at Ser62, which serves as a priming site for GSK-3 phosphorylation of Thr58	Nuclear target
DUSP6	44	Downstream effectors of Erk-MAPK pathways; involved in Erk negative feedback loop	Downstream target
Beta actin	45	Loading control	Loading control

482

483

484 **Supplementary Table S6: Clinically achievable concentrations, metabolic**
485 **and MAPK activity IC50, zebrafish embryos tested concentrations, and**
486 **MTDs**
487

Clinical data		BT40		DKFZ-BT66_ON		DKFZ-BT66_OFF		Zebrafish embryos		
Cmax (nM)	Ctrough (nM)	Metabolic IC50 (nM)	MAPK IC50 (nM)	Metabolic IC50 (nM)	MAPK IC50 (nM)	Metabolic IC50 (nM)	MAPK IC50 (nM)	Concentration range tested (nM)	MTD (nM)	LD (nM)
4 892.3	3 461.6	62.7	12.7	NA	8.5	NA	8.0	1 - 50 000	2 500	25 000
Ulixertinib 6,adult										
19.2	3.6	2.2	0.3	NA	2.1	NA	0.5	0.1 - 50 000	100	1 000
Trametinib 7, ped.										
1 296.0	ND	259.3	6.1	NA	164.1	NA	13.0	5 - 2 500	> 2 500	> 2 500
Selumetinib 8, ped.										
619.0	136.0	200.2	4.5	NA	88.0	NA	9.2	5 - 5 000	> 5 000	> 5 000
Binimetinib 9, adult										
ND	ND	112.3	NA	7.4	NA	1.6	NA	NA	ND	ND
A-1331852										
994.2	400.0	462.2	NA	324.9	NA	37.2	NA	1 - 50 000	10 000	50 000
Navitoclax 10,adult+ped										
1 612.1	725.4	NA	NA	2 991.0	NA	2 460.0	NA	0.1 - 10 000	10 000	>10 000
Venetoclax 10,adult+ped										
30.8	ND	2.9	NA	5.2	NA	6 591.0	NA	5 - 65 000	5 000	25 000 000*
Vinblastine 11,ped										
58 989.9	ND	62 593.0	NA	88 652.0	NA	97 169.0	NA	ND	ND	ND
Carboplatin 12,ped										

NA: Not applicable
 ND: Not determined

* slight toxicity, not
 lethal

488 **Supplementary Table S7: Navitoclax concentrations *in vivo* in PDX-BT40**
 489 **tumor tissue as measured by UPLC-MS/MS**

Animal ID	Treatment group	Navitoclax concentration [ng/g]
#1	Navitoclax monotherapy	3930
#3	Navitoclax monotherapy	232
#4	Navitoclax monotherapy	99
#5	Navitoclax monotherapy	1980
#6	Navitoclax monotherapy	1910
#7	Navitoclax monotherapy	118
#9	Ulixertinib + navitoclax combination	1960
#10	Ulixertinib + navitoclax combination	146
#11	Ulixertinib + navitoclax combination	111
#13	Ulixertinib + navitoclax combination	191
#15	Ulixertinib + navitoclax combination	3.7
#16	Ulixertinib + navitoclax combination	25

490 In green are concentrations higher than the effective concentration; in red concentrations
 491 lower than the effective concentration (effective concentration: *in vitro* metabolic activity IC₅₀
 492 in BT40 = 462.2 nM = 0.45 µg/mL).

493

494 **Supplementary Table S8: Drugs conditions for *in vitro* assays**

Drug name	Supplier	Cat. No.	Stock concentration (mM)	Class	Solvent	Storage
Ulixertinib	BioMed Valley Discoveries	NA	50	ERK inhibitor	DMSO	-80°C
Trametinib	Selleckchem	S2673	10	MEK inhibitor	DMSO	-80°C
Selumetinib	Selleckchem	S1008	10	MEK inhibitor	DMSO	-80°C
Binimetinib	Selleckchem	S7007	10	MEK inhibitor	DMSO	-80°C
Navitoclax	Selleckchem	S1001	50	Senolytic	DMSO	-80°C
Venetoclax	Selleckchem	S8048	10	Senolytic	DMSO	-80°C
A-1331852	Selleckchem	S7801	10	Senolytic	DMSO	-80°C
Vinblastine	MedChemExpress	HY-13780	10	SOC chemotherapy	DMSO	Room temperature under nitrogen atmosphere
Carboplatin	Pharmacy of the university hospital of Heidelberg	NA	25	SOC chemotherapy	Saline solution	4°C (away from light)
Staurosporine	TargetMol	T16680	10	Protein kinase inhibitor (death control)	DMSO	-80°C

496 **Supplementary Table S9: CellProlifer pipelines for high content**

497 **microscopy analysis**

498 (See Excel file)

499

500 **Supplementary Table S10: Drugs and solvents used in BT40-PDX mouse**
 501 **model in vivo**

Drugs	Concentration (mg/kg)	Solvent	Cat. No.	Supplier
Ulixertinib	75-80	1% CMC	NA	BioMed Valley Discoveries
Navitoclax ¹³	100	10% Ethanol 30% Polyethylen- glycol 400 60% Phosal 50	201970	MedKoo Biosciences
Vinblastine ¹⁴	0.5	0.9% NaCl	S4505	Selleckchem

502

Solvents	Cat. No.	Supplier
Carboxymethylcellulose (CMC sodium - medium viscosity)	C4888	Sigma-Aldrich
Ethanol	32205	Sigma-Aldrich
Polyethylenglycol 400	0144.1	Carl Roth
Phosal 50	368315	Lipoid
NaCl	2350748	B.Braun

503

504

505 **Supplementary Table S11: Optimized MS/MS parameters for the**
506 **detection of ulixertinib using heated electrospray ionization and selected**
507 **reaction monitoring in the positive ion mode**

Parameter	Value
Capillary voltage [kV]	1
Cone voltage [V]	50
Source temperature [°C]	150
Desolvation temperature [°C]	500
Cone gas (N2) flow [L/h]	150
Desolvation gas (N2) flow [L/h]	1000
Ulixertinib mass transition [<i>m/z</i>]	433.2 à 262.1
D7-ulixertinib mass transition [<i>m/z</i>]	439.2 à 268.1
Collision gas (Ar) flow [mL/min]	0.15
Collision energy [V]	16

508

509 **Supplementary Table S12: Optimized MS/MS parameters for the**
510 **detection of navitoclax using heated electrospray ionization and selected**
511 **reaction monitoring in the positive ion mode**

Parameter	Value
Capillary voltage [kV]	1.2
Cone voltage [V]	20
Source temperature [°C]	150
Desolvation temperature [°C]	600
Cone gas (N2) flow [L/h]	150
Desolvation gas (N2) flow [L/h]	1000
Navitoclax mass transition [<i>m/z</i>]	487.5 à 742.0
Venetoclax mass transition [<i>m/z</i>]	434.8 à 636.2
Collision gas (Ar) flow [mL/min]	0.15
Collision energy [V]	14

512

513 **Supplementary References**

- 514 1. Castro F, Dirks WG, Fähnrich S, Hotz-Wagenblatt A, Pawlita M, Schmitt M.
515 High-throughput SNP-based authentication of human cell lines. *Int J Cancer*.
516 2013;132(2):308. doi:10.1002/IJC.27675
- 517 2. Schmitt M, Pawlita M. High-throughput detection and multiplex identification of
518 cell contaminations. *Nucleic Acids Res*. 2009;37(18):e119.
519 doi:10.1093/NAR/GKP581
- 520 3. Wrobel JK, Najafi S, Ayhan S, et al. Rapid In Vivo Validation of HDAC Inhibitor-
521 Based Treatments in Neuroblastoma Zebrafish Xenografts. *Pharmaceuticals*.
522 2020;13(11):1-20. doi:10.3390/PH13110345
- 523 4. Committee for Medicinal Products for Human Use, European Medicines
524 Agency, Guideline on validation of bioanalytical methods
525 EMEA/CHMP/EWP/192217/2009. Published 2009. Available at
526 [http://www.ema.europa.eu/docs/en_GB/document_library/Scientific_guideline/2](http://www.ema.europa.eu/docs/en_GB/document_library/Scientific_guideline/2011/08/WC500109686.pdf)
527 [011/08/WC500109686.pdf](http://www.ema.europa.eu/docs/en_GB/document_library/Scientific_guideline/2011/08/WC500109686.pdf). Accessed November 2021.
- 528 5. US Department of Health and Human Services, Food and Drug Administration,
529 Guidance for Industry, Bioanalytical Method Validation. Published 2018.
530 Available at
531 [http://www.fda.gov/downloads/Drugs/GuidanceComplianceRegulatoryInformati](http://www.fda.gov/downloads/Drugs/GuidanceComplianceRegulatoryInformation/Guidances/ucm070107.pdf)
532 [on/Guidances/ucm070107.pdf](http://www.fda.gov/downloads/Drugs/GuidanceComplianceRegulatoryInformation/Guidances/ucm070107.pdf). Accessed November 2021.
- 533 6. Sullivan RJ, Infante JR, Janku F, et al. First-in-Class ERK1/2 Inhibitor
534 Ulixertinib (BVD-523) in Patients with MAPK Mutant Advanced Solid Tumors:
535 Results of a Phase I Dose-Escalation and Expansion Study. *Cancer Discov*.
536 2018;8(2):184-195. doi:10.1158/2159-8290.CD-17-1119

- 537 7. Cox DS, Allred A, Zhou Y, et al. Relative bioavailability of pediatric oral solution
538 and tablet formulations of trametinib in adult patients with solid tumors. *Clin*
539 *Pharmacol Drug Dev.* 2015;4(4):287-294. doi:10.1002/CPDD.152
- 540 8. Fangusaro J, Onar-Thomas A, Poussaint T, et al. Selumetinib in Children with
541 BRAF-Aberrant or Neurofibromatosis type 1-Associated Recurrent, Refractory
542 or Progressive Low-Grade Glioma: a Multi-Center Phase II Trial. *Lancet Oncol.*
543 2019;20(7):1011. doi:10.1016/S1470-2045(19)30277-3
- 544 9. Bendell JC, Javle M, Bekaii-Saab TS, et al. A phase 1 dose-escalation and
545 expansion study of binimetinib (MEK162), a potent and selective oral MEK1/2
546 inhibitor. *Br J Cancer* 2017 1165. 2017;116(5):575-583.
547 doi:10.1038/bjc.2017.10
- 548 10. Pullarkat VA, Lacayo NJ, Jabbour E, et al. Venetoclax and navitoclax in
549 combination with chemotherapy in patients with relapsed or refractory acute
550 lymphoblastic leukemia and lymphoblastic lymphoma. *Cancer Discov.*
551 2021;11(6):1440-1453. doi:10.1158/2159-8290.CD-20-
552 1465/333563/AM/VENETOCLAX-AND-NAVITOCCLAX-IN-COMBINATION-
553 WITH
- 554 11. Stempak D, Gammon J, Halton J, Moghrabi A, Koren G, Baruchel S. A pilot
555 pharmacokinetic and antiangiogenic biomarker study of celecoxib and low-dose
556 metronomic vinblastine or cyclophosphamide in pediatric recurrent solid
557 tumors. *J Pediatr Hematol Oncol.* 2006;28(11):720-728.
558 doi:10.1097/01.MPH.0000243657.64056.C3
- 559 12. Riccardi R, Riccardi A, Lasorella A, et al. Clinical pharmacokinetics of
560 carboplatin in children. *Cancer Chemother Pharmacol* 1994 336.

- 561 1994;33(6):477-483. doi:10.1007/BF00686504
- 562 13. Tse C, Shoemaker AR, Adickes J, et al. ABT-263: A Potent and Orally
563 Bioavailable Bcl-2 Family Inhibitor. *Cancer Res.* 2008;68(9):3421-3428.
564 doi:10.1158/0008-5472.CAN-07-5836
- 565 14. Klement G, Baruchel S, Rak J, et al. Continuous low-dose therapy with
566 vinblastine and VEGF receptor-2 antibody induces sustained tumor regression
567 without overt toxicity. *J Clin Invest.* 2000;105(8):R15. doi:10.1172/JCI8829
- 568